Cell Reports
Medicine

Article

The complex molecular epileptogenesis landscape of glioblastoma

Graphical abstract

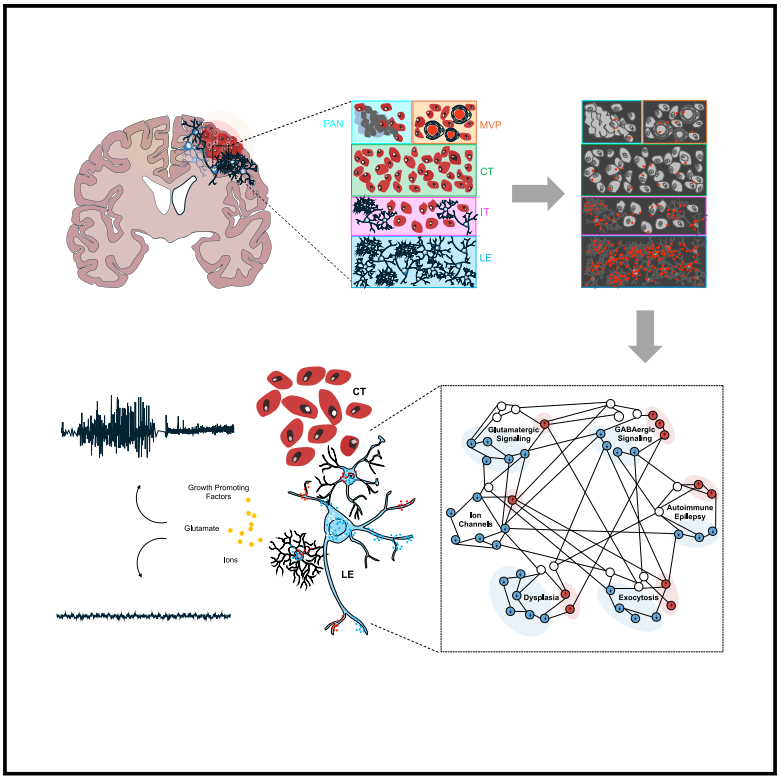

Authors

Victoria Soeung, Ralph B. Puchalski, Jeffrey L. Noebels

Correspondence

jnoebels@bcm.edu

In brief

Soeung et al. report spatial analysis of monogenic epilepsy-linked gene expression in human glioblastoma. The dysregulated genes affect multiple molecular pathways, and their dose-dependent and epistatic interactions explain both the presence and absence of seizures in individual patients, as well as the basis for pharmacoresistance to narrowly targeted antiseizure drugs.

Highlights

- 157 genes linked to human monogenic epilepsy are enriched at the tumor leading edge
- Dosage-sensitive dysregulation of multiple gene pathways validates proepileptogenicity
- Leading edge epilepsy-linked genes recapitulate early developmental expression patterns
- Epistatic genetic remodeling defines a basis for pharmacoresistant epilepsy therapy

Soeung et al., 2024, Cell Reports Medicine *5*, 101691
August 20, 2024
https://doi.org/10.1016/j.xcrm.2024.101691

CellPress

Cell Reports Medicine

CellPress
OPEN ACCESS

Article

The complex molecular epileptogenesis landscape of glioblastoma

Victoria Soeung,[1] Ralph B. Puchalski,[3] and Jeffrey L. Noebels[1,2,4,*]
[1]Developmental Neurogenetics Laboratory, Department of Neurology, Baylor College of Medicine, Houston, TX, USA
[2]Center for Cancer Neuroscience, Baylor College of Medicine, Houston, TX, USA
[3]Ben and Catherine Ivy Center for Advanced Brain Tumor Treatment, Swedish Neuroscience Institute, Seattle, WA, USA
[4]Lead contact
*Correspondence: jnoebels@bcm.edu
https://doi.org/10.1016/j.xcrm.2024.101691

SUMMARY

The cortical microenvironment surrounding malignant glioblastoma is a source of depolarizing crosstalk favoring hyperexcitability, tumor expansion, and immune evasion. Neosynaptogenesis, excess glutamate, and altered intrinsic membrane currents contribute to excitability dyshomeostasis, yet only half of the cases develop seizures, suggesting that tumor and host genomics, along with location, rather than mass effect, play a critical role. We analyzed the spatial contours and expression of 358 clinically validated human epilepsy genes in the human glioblastoma transcriptome compared to non-tumor adult and developing cortex datasets. Nearly half, including dosage-sensitive genes whose expression levels are securely linked to monogenic epilepsy, are strikingly enriched and aberrantly regulated at the leading edge, supporting a complex epistatic basis for peritumoral epileptogenesis. Surround hyperexcitability induced by complex patterns of proepileptic gene expression may explain the limited efficacy of narrowly targeted antiseizure medicines and the persistence of epilepsy following tumor resection and clarify why not all brain tumors provoke seizures.

INTRODUCTION

Pathological cortical hyperexcitability in the glioblastoma microenvironment is both an early warning and a lasting clinical legacy of this aggressive brain cancer. Seizures are the presenting sign in nearly one-half of patients with glioblastoma, may promote tumor growth, and typically persist as pharmacoresistant epilepsy after tumor resection,[1] indicating a sustained restructuring of network excitability in the surrounding host neocortex. While mechanisms underlying acquired peritumoral epileptogenesis and its impact on malignant cell invasion, cognitive impairment, and survival are under active exploration,[2] correcting this deleterious outcome, particularly in view of treatment advances prolonging survival,[3] remains a foremost goal in the clinical management of brain tumors.

The early pathophysiology of tumor-related epilepsy (TRE) is not fully explained by mass effect. While edema and increased intracranial pressure might contribute at later stages, persistence following tumor resection indicates that tissue compression alone is not required, and the large fraction of cases without a seizure history supports the inference of genetic risk as a principal component. Recent evidence in preclinical mouse glioblastoma models reveals that peritumoral synaptic imbalance and cortical hyperexcitability are determined by the specific oncogenes selected to drive tumor formation[4] as well as intrinsic susceptibility to epilepsy,[5] pointing to a process of gradual network remodeling typical of acquired focal epileptogenesis that depends upon tumor and host genomics and cortical location rather than the space-occupying mass.

While little is known about the *in situ* electrobiology of human brain tumors prior to their clinical detection, serial studies of tumor progression in a new generation of *in utero* electroporation (IUE) mouse glioblastoma models are providing key insights into tumor epileptogenesis. In these immunocompetent, coisogenic tumor models, hyperexcitability onset coincides with the emergence of tumor cell subclones expressing mRNA profiles enriched with synapse-related genes.[6] Alternative IUE tumor driver genes significantly determine the TRE phenotype, and epileptic tumors show a high ratio of excitatory to inhibitory synaptic markers in the tumor margin absent in non-epileptic tumors.[4,7] Peritumoral network remodeling during this period is also accompanied by a sequential loss of fast-spiking interneurons, perineuronal nets, altered glutamate exporter expression, microglial activation,[5] and the emergence of glutamate-linked microcircuit hyperactivity.[8] These defects confirm earlier observations in immunodeficient xenograft models,[9,10] indicating they arise independently of changes in the adaptive immune landscape.[11]

Far more is known about the gene determinants of cortical seizures in the absence of brain tumor. Over 350 genes are causally linked to monogenic epilepsy by virtue of their *de novo* recurrence in patients and populate clinical exome screening panels in wide use for precision epilepsy diagnosis.[12] These clinically validated risk genes encode a broad array of ion channel subunits, transporters, synaptic proteins, and neuronal migration factors, as well as oncogenic and intracellular metabolic pathways,[13] invoking a spectrum of candidate network excitability

mechanisms ranging from fast (msec) synaptic activity to slow (minutes) paracrine signaling and ultraslow (hours) transcriptional dysregulation. Both gain and loss-of-function mutations in many of these genes are pathogenic, and, in some, haploid dose alterations are also sufficient. To date, only a few candidate genes have been implicated by differential expression in bulk low-grade gliomas,[14,15] but without spatial resolution or validation of a direct role in intact human network hyperexcitability.[16,17] Given the biologically diverse pathways and molecular plasticity within glioma microniches during tumor evolution,[18] the relative contribution of any single one of these genes to epileptic network synchronization is unclear, and a simultaneous large-scale spatial mapping of their regulated expression, case concordance, and fold change relative to unaffected developing and adult neocortex has not yet been performed.

Here, we analyze the mRNA expression of 358 genes for human monogenic epilepsy (Epi358) according to their anatomical expression in human spatial and developmental transcriptome databases (see methods for details). The extended analysis includes epilepsy gene sets linked to channelopathies, receptors, transporters, exocytotic release, familial migraine with seizures, molecular targets of autoimmune epilepsies, and somatic gene mutations leading to epileptic focal cortical dysplasia. Our analysis reveals pathogenic patterns of spatial enrichment and extensive dysregulation of epilepsy-linked genes at the tumor leading edge (LE) when compared to the pure tumor cell region and the healthy cortex. Across functional clusters, the transcription profiles of genes for ion homeostasis and macromolecular biosynthesis most closely resemble those in developing unaffected cortex. The microvascular zone of tumor cell proliferation and migration encompassing the blood-brain barrier (BBB) is the second most dysregulated region of proepileptogenic genes. Most other tumor cell regions show little significant enrichment compared to the pure cellular tumor. These complex patterns of coordinate dysregulation may allow more precise matching of tumor molecular excitability subtypes with antiseizure medicines to direct future gene-guided clinical management of glioblastoma.

RESULTS

Monogenic sources of epileptogenesis aggregate at the tumor LE

To characterize the intratumoral heterogeneity of epilepsy-linked genes, we first determined the comparative enrichment ratios (ERs) of epilepsy gene transcripts for 6 anatomically and molecularly defined tumor regions compared to the pure cellular tumor (CT)[19] (see Methods). Our analysis reveals the distinct arealization of the excitability transcriptome and highlights the spatial heterogeneity across tumor regions (Figure 1A). We found a large proportion (157/358) of epilepsy genes enriched by 1.5-fold or higher at the LE (containing only 1%–3% tumor cells), a similar fraction (172/358) without significant change, and an interesting subset (25/358) enriched in pure tumor cell regions relative to the LE (high-resolution details in Figure S1; Table S1). At the LE-adjacent infiltrating tumor (IT) (containing 10%–20% tumor cells), 118/358 genes are enriched but to a lesser magnitude as expected by the lower neuronal content of this region. Other intratumoral regions each contain less than 50 enriched genes as compared to the CT. In contrast, both the LE and IT also contain the fewest under-enriched genes (25/358 and 2/358, respectively), while the microvascular proliferation (MVP) region contains the most under-enriched genes within the tumor (113/358). Genes enriched at the LE have the highest statistical significance and case concordance (Figure S1; Table S1). Only 19% of Epi358 genes show low concordance at the LE (67/358), and concordance is lower in other regions consistent with tumor cell heterogeneity. To assess whether seizure status altered regional RNA expression levels, we compared RNA expression between cases presenting with seizures and those without (FC_{sz}) (Figure S2; Table S1). We found that despite a greater than 10-fold elevation (FC_{sz}) of *FOSB*, an immediate-early gene sensitive to excess neuronal depolarization, relatively few Epi358 genes are consistently amplified over 2-fold by a history of seizures in this cohort.

Heterogeneous proepileptic pathways are enhanced in distinct intratumoral zones

We then conducted a Gene Ontology analysis to classify the Epi358 genes by biological processes and identified three major categories, (1) cell growth and division (CGD), (2) ion channel and transporter (ICT), and (3) macromolecule biosynthesis (MBS) (Figure 1B). Intriguingly, 81% of the genes in the ICT category are enriched at the LE, whereas the majority of MBS genes show equivalent expression at the LE and CT. Approximately 50% of genes in the CGD category are enriched only at the LE while the other half are expressed equally between the LE and CT (Figure 1C). Thus, a significant number of epilepsy-linked genes show specific enrichment at the LE, and their dysregulated expression would be masked in a bulk tumor analysis (Figure 1D). For example, both deletions and heterozygous missense mutations of *SNAP25*, a key regulator of transmitter exocytosis, are proepileptic.[20] Despite the low level originally reported in bulk human glioma suggesting a role in tumor suppression,[21] we found that *SNAP25* is markedly enriched and upregulated at the LE consistent with a high peritumoral synaptic density but is not enriched in deep tumor regions (Figure S1), where, in the absence of significant synaptic connectivity, it is unlikely to contribute to aberrant network activity. Another instructive example is *LGI1*, a gene so named upon its discovery in bulk tissue as "low in glioma."[22] *LGI1* was initially considered a putative glioma suppressor with no known role in excitability, yet it is now recognized as a presynaptic protein linked to potassium channel function[23] and autoimmune epilepsy.[24] We consistently find *LGI1* strongly enriched and upregulated (Figure S1) at both the LE and IT but not in other tumor regions. Thus, genes may exert congruent or opposing network excitability and growth-promoting effects, either singly or as a composite group, in different spatial contexts that may be obscured in bulk tissue analyses.

Tumor lobar location does not greatly affect dysregulation of Epi358 genes at the LE

Next, we ascertained the relative magnitude of dysregulation at the cortical tumor margin by comparing the mean expression of the Epi358 genes at the LE to expression levels in anatomically

CellPress
OPEN ACCESS

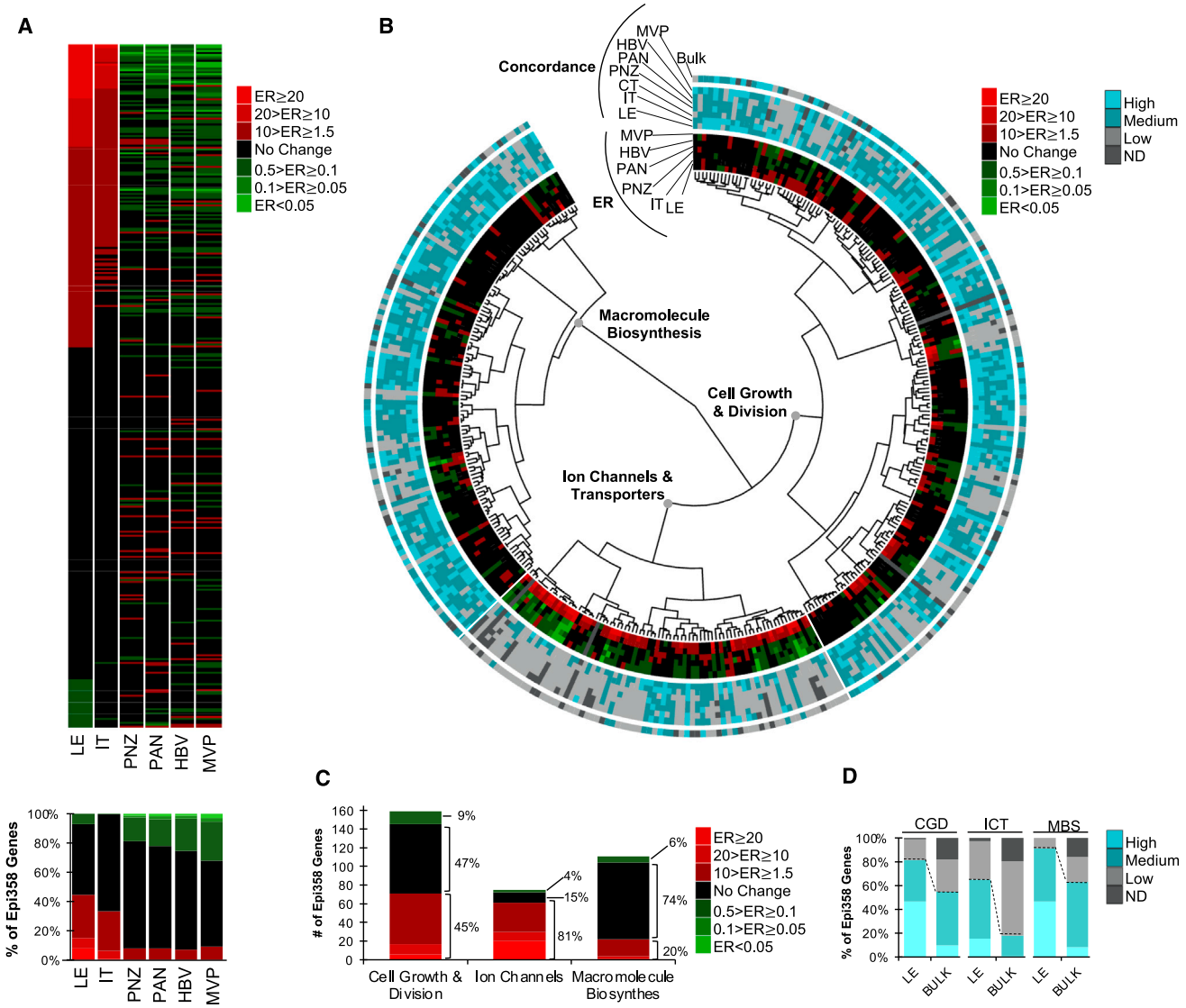

Figure 1. Monogenic sources of epileptogenesis aggregate at the tumor LE

(A) The LE is enriched for monogenic sources of epileptogenesis. Upper: heatmaps ordered by magnitude of enrichment at the LE compared to cellular tumor zone. Nearly 50% of monogenic sources of epilepsy are either enriched specifically at the LE (157/358) or equally expressed in the LE and CT (172/358). Lower: percent of cases enriched in each zone. Detailed gene list given in Figure S1.

(B) Epi358 genes are involved in diverse cellular processes. Circular tree plot of the Epi358 genes based on hierarchical clustering by biological function. Inner circle: Gene Ontology analysis defined three broad categories: (1) cell growth and division (CGD), (2) ion channel and transporter (ICT), and (3) macromolecule biosynthesis (MBS). Middle circle: the enrichment ratio (ER) for genes in the ICT category is almost exclusively enriched at the LE. Outer circle: regional RNA-seq results in improved concordance for all categories compared to bulk tumor analysis. Detailed gene list given in Figure S1.

(C) Epilepsy-linked ion channels show the strongest enrichment at the LE. Bar plot quantifying the enrichment status of Epi358 genes at the LE compared to the CT. A large percentage of genes in the CGD category and greater than 80% of genes in the ICT category show strong LE enrichment.

(D) Case concordance at the LE is greater for all functional categories as compared to bulk analysis. Bar plot quantifying concordance of gene expression of Epi358 genes at the LE as compared to concordance from bulk tumor analysis. For genes in the CGD and MBS categories, there were 1.49-fold and 1.44-fold more genes that display high-medium concordance at the LE compared to bulk analysis, respectively. Genes in the ICT category show the most improved case concordance as compared to bulk tumor analysis with 3.57-fold more genes with high-medium concordance at the LE.

aligned, age-matched, healthy human frontal, temporal, or parietal lobe cortical samples published in the Human Protein Atlas database.[25] The majority of genes show altered expression levels at the LE compared to non-tumor cortex, suggesting that although the neuronal, glial, and immune cells at the LE are microscopically similar to healthy cortex, they are highly transcriptionally remodeled. The Epi358 genes fall into multiple distinct groups according to their intratumoral ER and fold change (FC_{Cx}) profile per cortical lobe (Figure 2A, groups 1–15). Intriguingly, the majority of epilepsy-linked transcripts

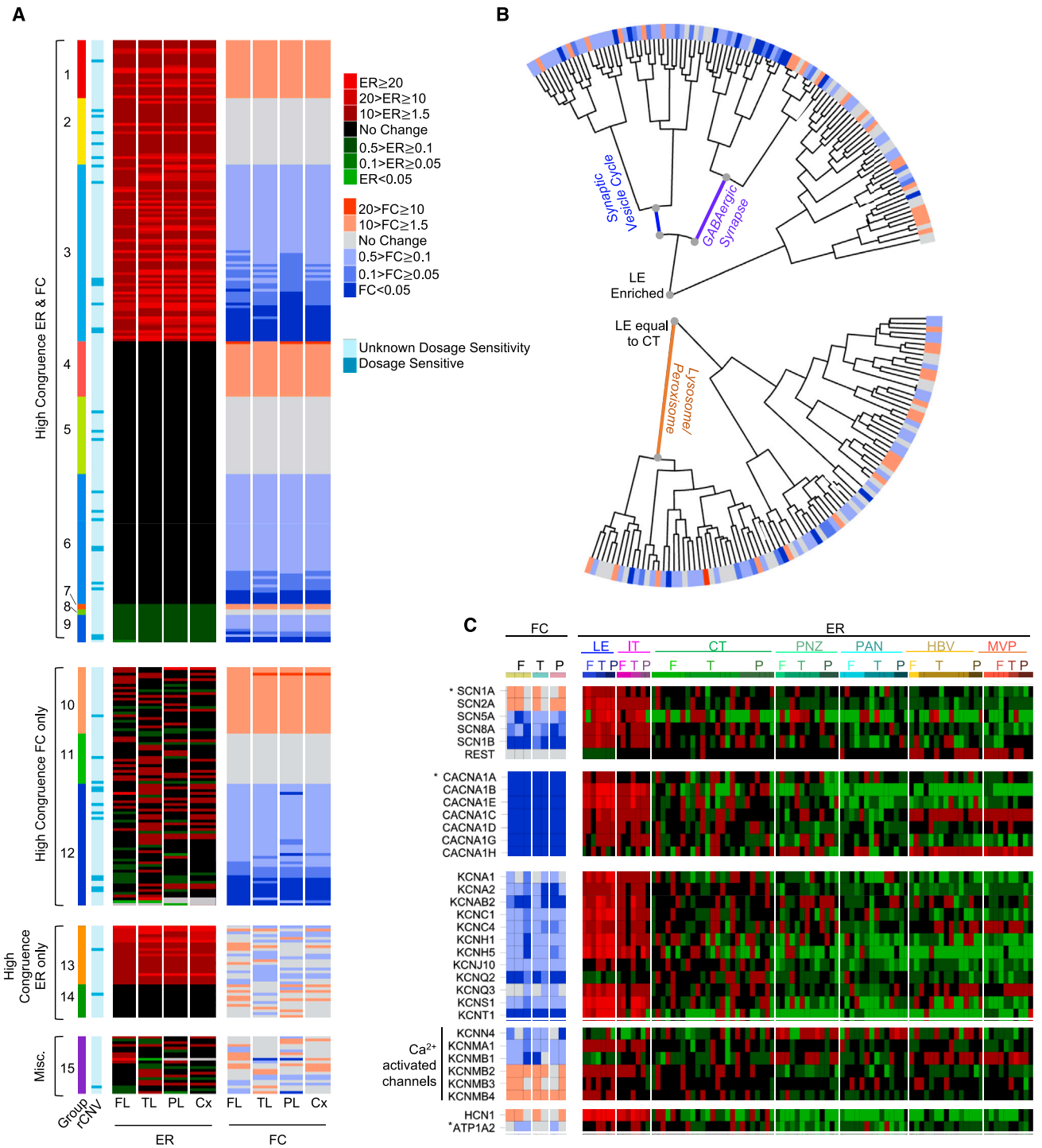

Figure 2. Complexity and degree of dysregulation support an epistatic basis of epileptogenesis at the LE

(A) The majority of genes linked to monogenic epilepsy are similarly dysregulated across the frontal, temporal, and parietal lobes. Heatmap of the ER and FC_{Cx} of Epi358 genes at the LE compared to different lobes of healthy human cortex. Lanes show samples from the frontal (FL), temporal (TL), parietal (PL) lobes, and pooled cortex (Cx). The expression patterns were stratified according to congruence of ER and FC of tumors derived from different cortical lobes, forming 15 distinct groups (color coded). Groups 1–9 share a similar FC_{Cx} and ER pattern at the LE, whereas groups 10–12 and 13–14 share only a similar FC_{Cx} or ER pattern, respectively. Group 15 genes show a variable ER and FC_{Cx} pattern. Forty-one of the Epi358 are validated pathogenic dosage-sensitive genes (rCNVs) (see Figure S3 for more details on the 41 epilepsy-linked rare copy-number variants; rCNVs).

(legend continued on next page)

show a high congruence between ER and FC_{Cx} despite the different locations of the cortical tumors (Figure 2A, 218/358, groups 1–9). Another large subset (Figure 2A, 85/358, groups 10–12) shows high congruence of fold change relative to the native cortex but differs in intratumoral enrichment profile. The high congruence of FC_{Cx} across cortical regions suggests that for these epilepsy-linked genes, the tumor is similarly remodeling the LE despite any intrinsic differences in the surrounding cortical tissue. However, lobar synaptic connectivity differences adjacent to the LE may also contribute to why some tumors provoke peritumoral epilepsy.

Complexity and degree of LE dysregulation support an epistatic basis of epileptogenesis

We further characterized the 218 genes that showed high congruence of dysregulation at the LE across the frontal, temporal, and parietal lobes (groups 1–9). We conducted a Gene Ontology analysis to cluster the genes according to similar biological function for groups 1–3 (enriched at the LE) and groups 4–6 (equal LE and CT expression), respectively (Figure 2B), and then conducted a Kyoto Encyclopedia of Genes and Genomes (KEGG) pathway analysis of major clusters of these genes. Our analysis shows striking dysregulation of multiple genes involved in neuronal functions such as synaptic vesicle cycle and GABAergic synaptic function at the LE. Although the majority of genes are downregulated compared to healthy cortex, a subset in each pathway is aberrantly upregulated. Similar to the genes enriched at the LE, those in group 4–6 show high dysregulation, with a large proportion downregulated and a few aberrantly upregulated. Overall, the transcriptome profile at the LE differs greatly from region- and age-matched healthy cortex, indicating a complex dysregulation of multiple pathways and an epistatic basis for peritumoral hyperexcitability and epileptogenesis.

Dosage-sensitive genes validate the pathogenicity of large fold changes at the LE

Although transcript-level changes only provide plausible evidence of actual functional impact, many heterozygous nonsense or missense mutations that lead to an equivalent loss or gain of function cause seizures in patients,[26] and the experimental literature is replete with overexpression and haploinsufficient seizure models based on gene dosage. Important human examples of epilepsy-linked dosage-sensitive genes include *SCN1A*, *SCN2A*, *CHD2*, *SYNGAP1*, and *DEPDC5.* We determined that 41 of the Epi358 genes are known dosage-sensitive genes, where allele haploinsufficiency and/or triplosufficiency in non-tumor brain lead to epilepsy in human patients (Figure 2A second column, genes listed in Figure 3). Aberrant dosage of any of these genes alone is sufficient evidence of pathogenicity. We therefore adopted a level of 0.5- and 1.5-fold change in transcript density as a benchmark for prioritizing pathogenicity. We found that 16/25 haploinsufficient genes are downregulated, and 2/26 triplosensitive genes are upregulated at the LE (Figures S3A and S3B). Thus, 18/41 dosage-sensitive genes that have been independently linked to clinical seizure and neurodevelopmental disorders show dysregulated expression profiles sufficient for clinical expression of epileptogenesis at the LE.

Homeostatic mechanisms of ion equilibrium are pathologically remodeled at the LE

Ion channelopathy is the best understood class of monogenic epilepsy, and each channel is linked to multiple variant-defined clinical syndromes. We found that of the three major functional gene categories, only the ICT group contains a majority of genes that are enriched and dysregulated at the LE (Figures S3C–S3E). Detailed functional and computational analyses in both heterologous cells and *in situ* cortical networks have established that pathogenic channel variants with slight to major shifts in either biophysical activation or deactivation properties lead to a range of epilepsy phenotypes and antiepileptic drug sensitivities. Similarly, impaired interactions with their regulatory subunits reproduce current defects across many channel subtypes.[27] The epistatic consequences of multiple gain or loss-of-function variants are complex due to the cell type-specific roles of ion channels in sculpting excitability within synaptic microcircuits. The combinatorial outcome of even two distinct epilepsy gene mutations on a seizure phenotype depends on the specific network affected and may either exacerbate or attenuate network hyperexcitability.[28,29] We find extensive levels of transcriptional dysregulation within all major classes of voltage-gated ion channels (details are in the following paragraph), highlighting the tumor-induced departure from homeostatic mechanisms maintaining excitatory and inhibitory equilibrium in the surrounding cortical circuitry.

Sodium channels are enriched and dysregulated at the LE

Voltage-gated sodium channels mediate depolarization in response to changes in membrane potential, enabling the initiation and propagation of action potentials. Four pore-forming alpha subunits linked to epilepsy, *SCN1A*, *2A*, *5A*, and *8A*, and the regulatory subunit *SCNB1* are all significantly enriched at the LE and decreased elsewhere in the tumor (Figure 2C). However, only *SCN1A* and *SCN2A* have elevated expression compared to healthy cortex, whereas *SCN5A*, *8A*, and *SCNB1* have reduced expression. Experimental studies of epilepsy-linked clinical variants of these sodium channels indicate that either gain or loss of function can contribute to network hyperexcitability. Coordinate changes in channel genes may also reflect local altered upstream transcription factors. For example, the

(B) Genes from groups 1–3 (LE enriched) and groups 4–6 (LE equal to CT) were hierarchically clustered according to biological function. KEGG pathway analysis of prominent clusters identified pathways dysregulated at the LE. The dysregulation of multiple epilepsy-linked genes involved in diverse pathways supports an epistatic basis for epileptogenesis at the LE.

(C) Simultaneous dysregulation of multiple voltage-gated ion channels disrupts ion homeostasis and supports pathological spreading depolarization. Heatmap of the FC_{Cx} and sample-wise regional ER for voltage-gated sodium channel (VGSC), voltage-gated calcium channel (VGCC), and voltage-gated potassium channel (VGKC) subunits linked to epilepsy. Of the VGSCs, only *SCN1A* and *SCN2A* are upregulated compared to wild type (WT). Almost all VGCC and VGKC are downregulated except for a few calcium-activated potassium channels. Asterisks (*) denotes genes implicated in clinical cases of spreading depolarization.

NRSF/REST transcription corepressor silences sodium channel transcription[30] and thus decreased *REST* levels at the LE favor elevated sodium channel transcripts at this location and suppression where *REST* is more highly elevated, particularly at the MVP (Figure 2C).

Calcium channels are enriched and uniformly downregulated at the LE

PQ, N, and R-type channels (*CACNA1A*, *CACNA1B*, and *CACNA1E*, respectively) mediate excitation-coupled vesicular release at central synapses. We consistently found peritumoral enrichment of these calcium channels (Figure 2C), along with enriched expression of requisite presynaptic exocytotic machinery genes (Figure S4A), consistent with the excess synaptogenesis at the tumor margin seen in experimental glioblastoma models,[4,7,31] yet all presynaptic calcium channels are uniformly downregulated compared to healthy cortex (Figure 2C). However if dysregulation of these channels is unequally distributed across a microcircuit of excitatory and inhibitory neurons, the resulting excitatory:inhibitory release imbalance can explain why both gain and loss-of-function variants in these subunits may result in epilepsy.[32] L-type calcium channels mediate excitation-transcription coupling but are uncommon causes of epilepsy; their genes, *CACNA1C* and *CACNA1D*, are enriched at both the LE and MVP zone (Figure 2C). Low-voltage-activated T-type calcium channel genes *CACNA1G* and *CACNA1H* mediate rebound bursting in thalamocortical circuits and, when elevated, promote[33] or, when lowered, prevent[34] generalized spike-wave seizures. Their downregulation at the LE is consistent with the absence of this specific aberrant electroencephalography (EEG) pattern in glioblastoma tumor cases.

Potassium channels are predominantly enriched and downregulated at the LE

Potassium channel subunits comprise the largest class of epilepsy channelopathy,[35] with both gain and loss of function leading to prominent epilepsy phenotypes.[36] These channels exhibit complex combinatorial control over compartmental membrane excitability in dendrites and axons,[37] are modulated by various factors (i.e., membrane voltage, calcium ions, G-protein-coupled receptor [GPCR] signaling, and/or ATP), and also mediate a diverse range of essential cellular functions, including cellular homeostasis and membrane polarization. A large subset of potassium channel genes is strongly enriched at the peritumoral LE (*KCNA1*,*2*; *KCNAB2*; *KCNC1*; *KCNH1*,*5*; *KCNS1*; *KCNT1)* compared to tumor regions (Figure 2C). In contrast, *KCNQ2*, a gene encoding the non-inactivating Kv7 M-current does not show strong enrichment for any tumor region. Most of these genes are downregulated at the LE compared to healthy cortex except for a subset of calcium-activated channels (Figure 2C). The calcium-activated potassium channel subunit *KCNMB1* is downregulated at the LE but enriched at the MVP, a region rich in actively migrating cells. In contrast, the subunits *KCNMB2*,*3*,*4* show strong enrichment and upregulated expression at the LE. In neurons, mutations of *KCNMB1* and *KCNMB4* lead to epilepsy, but their role in tumor cells is unknown. However, the related calcium-activated potassium channel, *KCNN4*, is involved in glioma cell migration.[38] The enriched expression of potassium channel subunits at the LE with a known role in both intrinsic excitability and cellular proliferation, so-called ‘‘oncochannelopathy genes,’’[39,40] merits further exploration.

Breakdown of peritumoral ion homeostasis facilitates pathological spreading depolarization

Overall, our results indicate that multiple genes from different ion channel classes are simultaneously dysregulated at the LE, facilitating the pathological breakdown of ion homeostasis. One such pathological event is spreading depolarization. Spreading depolarization (SD) is a slowly propagating pathological wave of neuronal and glial depolarization resulting from the breakdown of membrane ion homeostasis and is implicated in neurologic defects associated with brain tumor progression such as hypoxic brain injury and migraine aura syndromes.[41] This glioblastoma excitability biomarker was detected emanating from the tumoral LE of glioblastoma mouse models.[5,7] Three genes are linked to SD threshold in monogenic syndromes of familial hemiplegia (FHM1–3) with seizures, including PQ-calcium channel, *CACNA1A*, in FHM1, astrocytic sodium potassium ATPase, *ATP1A2*, in FHM2, and sodium channel, *SCN1A*, in FHM3. Functional studies indicate that gain-of-function mutations in *CACNA1A*[42] and loss-of-function mutations in *ATP1A2*[43] and *SCN1A*[44] lower SD threshold. All three genes are enriched at the LE (Figure 2C**)**, and downregulation of *ATP1A2* is consistent with *ATP1A2* loss-of-function mutations resulting in SD. Although *SCN1A* is upregulated at the LE, its functional levels depend on its regulatory subunit, *SCN1B*, which is strongly downregulated at the LE, highlighting the epistatic interactions between ion channel subunits. While gain-of-function mutations of *CACNA1A* are associated with increased synaptic glutamate release, we found a strong downregulation of *CACNA1A* at the LE (Figure 2C). However, transmitter release might be enhanced by upregulation of other ion channels such as *HCN1*. Hyperpolarization and ATP-activated cyclic nucleotide channels (HCNs) conduct mixed cation (predominantly K^+ and Na^+) pacemaker currents that regulate neuronal bursting, and a spectrum of mutations in *HCN1–4* has been identified in patients with epilepsy.[45] We show that *HCN1* transcripts are strikingly enriched and upregulated at the LE (Figure 2C; Table S1), leading the list of Epi358 channel genes. Interestingly, a search in the Ivy Glioblastoma Atlas Project (GAP) for the strongest enrichment of all ion channel genes at the LE identified *KCNS1*, a potassium channel linked to brain edema and increased intracranial pressure[46] but not yet linked to epilepsy (Figure 2C). This gene is strongly enriched at the LE and shows uniform downregulation compared to healthy cortex. Overall, the complex dysregulation of ion channel transcripts at the LE is supportive of a hyperexcitable environment conducive to SD and other dysfunctions of ion homeostasis.

Peritumoral remodeling of glutamatergic and GABAergic signaling promotes hyperexcitability

Glutamate receptors show subtype-specific regional dysregulation

Mesoscale imaging in experimental[8] and human glioblastoma[47] reveals extensive extracellular glutamate accumulation contributing to epilepsy,[48] tumor progression,[49,50] and cortical SD.[5] High levels of glutamate are likely supplied by tumor cells and

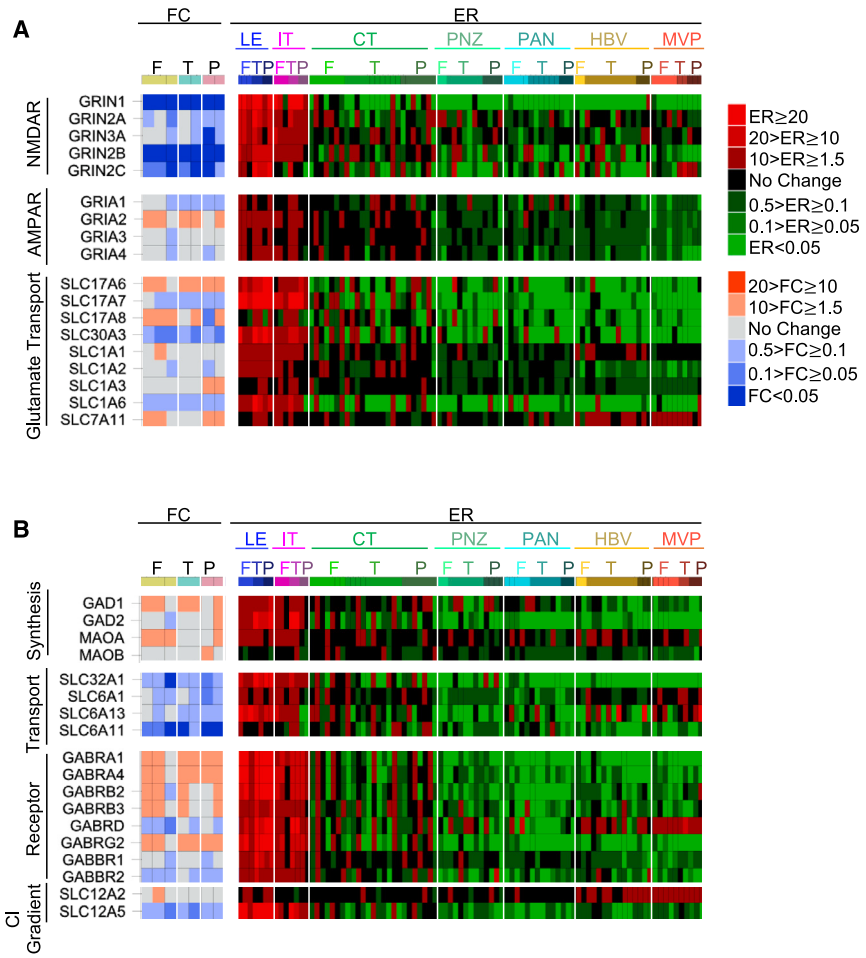

Figure 3. Peritumoral remodeling of glutamatergic and GABAergic signaling promotes hyperexcitability

(A) Dysregulation of glutamate signaling genes supports abnormal glutamate signaling and homeostasis. Ionotropic glutamate receptors show subtype-specific regional dysregulation. Although most NMDARs and AMPARs show strong enrichment at the LE, only *GRIA2* was upregulated, and most other glutamate receptors are downregulated in comparison to healthy cortex. Bottom: evidence for increased transcript levels of vesicular glutamate transport (*SLC17A6,8*) and astrocytic (*SLC7A11*) glutamate transporter.

(B) Dysregulation of GABA signaling genes supports abnormal GABA signaling favoring hyperexcitability. GABA synthesis genes are enriched and upregulated. GABA transport to and from the extracellular space are uniformly downregulated. GABA receptor dysregulation and chloride membrane gradient is conducive to depolarizing GABA signaling. GABA receptors display a subtype-specific upregulation at the LE. Although *SLC12A5* (*KCC2*) is uniformly enriched at the LE, it is consistently downregulated as compared to healthy cortex without a parallel increase in *SLC12A2* (*NKCC1*) expression, indicating a peritumoral *KCC2:NKCC1* ratio conducive to depolarizing GABA signaling.

astrocytes[51] and maintained by defective uptake,[52] but the involvement of receptors in this pathway has not been spatially resolved. We detected extensive LE enrichment of ionotropic (*NMDA/GRIN*, *AMPA/GRIA*), and metabotropic (*GRM*) glutamate receptor subunits relative to tumor regions (Figures 3A and S4B). NMDA (*GRIN1*, *2A*, *3A*, *2B*, and *2C*) receptor subunits concentrating at the LE suggest a mechanism for excitotoxicity; however, the FC_{Cx} values are uniformly depressed. In contrast, AMPA receptor (*GRIA1-4*) expression shows extensive LE and intratumoral enrichment consistent with a role in tumor growth,[53,54] although only *GRIA3* is so far genetically linked to epilepsy. *GRIA2* uniquely shows a major FC_{Cx} increase at the LE. Other members, including the extrasynaptic tonic glutamate receptor δ subunit gene *GRID1*, and kainate receptors show an elevated LE and tumor enrichment profile, yet a low FC_{Cx}. Metabotropic glutamate receptors (mGlur1–8) are strongly LE enriched and display subtype-specific downregulation compared to healthy cortex (Figure S4B). Mutations in these genes have not yet been linked to epilepsy.

Dysregulation of glutamate transport genes supports abnormal glutamate homeostasis

Synaptically releasable glutamate is concentrated in vesicles by proton-dependent (*VGLUT1–3/SLC17A6–8*) and zinc-dependent (*ZNT3/SLC30A3*) transporters. We found upregulation of the vesicular transporters, *SLC17A6* and *SLC17A8* at the LE, but not *SLC17A7* or *SLC30A3* (Figure 3A). Similarly, the astrocytic cysteine-glutamate exporter (*XCT/SLC7A11*) is enriched and upregulated at the LE and may also contribute to elevated extracellular glutamate levels[5] (Figure 3A). Three high-affinity neuronal and glial plasma membrane transporters (*SLC1A1–3*, *6*) are responsible for greater than 90% of cellular glutamate uptake in healthy brain and are all linked to epilepsy. These genes are LE enriched but expressed at healthy cortical levels (Figure 3A). The increased expression of glutamate exporters coupled with the lack of increase in cellular glutamate uptake may contribute to the excess glutamate accumulation seen in clinical and preclinical studies.

Evidence for increased GABA synthesis without parallel increase in transport

GABA, the primary inhibitory neurotransmitter, is synthesized from glutamate. Deficiencies in either *GAD1*[55] or *GAD2*[56] reduce inhibitory GABA signaling, and both are strongly LE enriched (Figure 3B). GABA can also be synthesized by outer mitochondrial membrane flavoenzymes, *MAOA* and *MAOB*. Like *GAD1*, *MAOA* is also elevated at the LE. However, contrary to *GAD1* deficiency, which can lead to seizures, duplication of *MAOA* has been reported in a patient with epilepsy.[57] Vesicular packaging of GABA by *VGAT/SLC32A1* and reuptake via plasma membrane transporters via *GAT1–3/SLC6A1,13,11* is strongly enriched at the LE but is largely downregulated at the LE compared to healthy cortex (Figure 3B).

GABA receptors show uniform LE enrichment and subtype-specific upregulation

Ionotropic GABA receptors are pentamers, and mutations in all subunits are linked to human epilepsies.[58] GABAergic transmission plays a critical role in network synchronization,[59] stem cell proliferation, migration, synaptogenesis, and immune cell function.[60,61] GABA receptors are reduced in bulk glioblastoma tumors compared to lower grade gliomas, and in deep glioblastoma tumor regions relative to the perimeter.[62] However, we detected uniform enrichment of all ionotropic α, β, and γ subunits at the LE compared to tumor cells, and a mixed FC_{Cx} pattern of receptor expression compared to healthy cortex (Figure 3B). Metabotropic GABA receptors (*GABBR1*,*2*) are also enriched at the LE. However, these genes are largely downregulated. Metabotropic GABA signaling is critical for epilepsy in non-malignant focal epileptic cortical dysplasia, including tuberous sclerosis.[63]

The peritumoral membrane chloride gradient is conducive to depolarizing GABA signaling

The effect of GABA on network excitability depends upon the postsynaptic transmembrane chloride gradient. This gradient undergoes a shift from depolarizing to hyperpolarizing during early brain development as chloride exporter, *KCC2* (*SLC12A5*), expression increases, reversing the balance of Cl^- import mediated by *NKCC1* (*SLC12A2*). *KCC2* loss-of-function mutations lead to epilepsy,[64] and a knockin mouse of a *KCC2* mutation that prevents phosphorylation-dependent inactivation suppresses convulsant-induced seizures,[65] validating the importance of this pathway and serving as a reminder of the critical role of posttranslational modulation for this and other genes. Analysis of chloride transport dysregulation in glioblastoma has yielded mixed results in human tissue and murine xenograft models.[66–68] However, we consistently found *KCC2* (*SLC12A5)* is enriched at the LE but downregulated compared to healthy cortex (Figure 3B) without a parallel increase in *NKCC1* (*SLC12A2*), indicating a *KCC2:NKCC1* ratio that favors depolarizing GABA signaling, which may contribute to peritumoral hyperexcitability.

The LE and MVP are distinct proepileptic zones

Our analysis identified the LE and MVP zone as the most proepileptic tumor regions (Figure 1A). A closer examination of the enrichment profile identified 32 epilepsy-linked genes enriched at the MVP zone compared with the CT (Figure 4A). Approximately half of those genes are also selectively enriched at the MVP compared to the LE and may influence neurovascular reactivity and BBB integrity.[69] For example, the mechanosensitive stretch non-selective cation channels *PIEZO1* and *PIEZO2* are exclusively enriched at the MVP (Figure 4B), and upregulation of both genes has been reported in a case of seizures with cortical compression.[70] While genomic variants are not as yet linked to genetic epilepsy, *THSN1*, the gene encoding astroglial thrombospondin1 was recently implicated in glioblastoma synaptic remodeling[31] and is also enriched at the MVP (Figure 4B). Pathological astroglial-based BBB alterations provide vasogenic mechanisms for local inflammation leading to hyperexcitability, as well as defective transport of antiepileptic drugs.[71]

Autoimmune epilepsy antigens are enriched at the LE

Autoimmune epilepsy is an uncommon result of pathogenic antibody binding to neuronal antigens leading to seizures[72] and typically diagnosed in the context of non-CNS cancers or no discoverable malignancy. Molecular targets of autoimmune antibodies include NMDA, AMPA, GABA, and glycine receptors (*GAD65*, *GAD67*, *LGI1*, *HU/ELAV4*, *NEUREXIN1–3*, and *CASPR2*[73]), and germline mutation of each of these targets is linked to monogenic epilepsy. Surprisingly, we found that genes for 22 autoimmune antigens show striking enrichment at the LE, while none are enriched at the MVP, pointing to an unexplored immunological pathway underlying glioblastoma-related epilepsy (Figure 4C). Glioblastoma is not currently recognized as one of the causative tumors underlying autoimmune epilepsy,[72,74,75] except in a single case report of seizures due to anti-glutamate receptor cerebral spinal fluid antibodies subsequently found to arise from an unrecognized glioblastoma,[76] suggesting this pathway merits further exploration.

Differences in the regulation of MTOR pathways at the LE and MVP

Mutations in genes of the *MTOR* pathway are one of the primary causes of focal cortical dysplasia (FCD), the most common cause of MRI-detectable, pharmacoresistant epilepsy. Somatic mutations of these genes generate localized cortical cell lineages and thus represent a model of non-malignant peritumoral epileptogenesis, and some (*KRAS*, *NF1*, *NIPBL*, and *PCDH19*) have been linked to cellular growth in glioblastoma.[77–79] We found that most *MTOR* pathway genes show lowered expression at the LE compared to healthy cortex, except for *NPRL2*, *KRAS*, and *PTEN*, which show increased expression (Figure 4D). Although *KRAS* and *PTEN* are upregulated, the *MTOR* repressors, *TSC1*, *TSC2*, *DEPDC5*, *NPRL3*, *RPTOR*, and *STRADA*, are all downregulated at the LE compared to healthy cortex, highlighting how different *MTOR* downstream pathways may be enhanced while others are repressed in glioblastoma (Figure 4D). *PTEN* is upregulated and enriched in both the LE and MVP regions, but the repressor *TSC1* is highly LE enriched yet downregulated at the LE, highlighting their different regional roles in tumorigenesis. *MTOR* inhibitors are effective antiseizure therapy for FCD and suppress glioblastoma tumor cell proliferation *in vitro*,[80] and their *in vivo* profile suggests further therapeutic study of the effects of *MTOR* signaling on glioblastoma-related epilepsy and tumorigenesis.

Epilepsy gene dysregulation at the LE partially recapitulates early development

Finally, we sought evidence for the important hypothesis that tumor-induced gene dysregulation may recapitulate patterns of plasticity characteristic of early cortical development.[81] We compared the degree of dysregulation of 254 Epi358 genes aberrantly expressed at the LE to healthy cortex during early prenatal and postnatal development (see Methods) and found that 54% of the LE dysregulated genes resemble a FC_{Cx} pattern similar to that of at least one early developmental stage (Figure 5A). Suppressors of *MTOR* signaling are uniformly downregulated at the LE and at all developmental stages tested (Figure 5B), suggesting that *MTOR* signaling itself is upregulated in both tumor LE and healthy cortex during these early developmental stages. Genes involved in neuronal migration are upregulated in healthy cortex at the prenatal and infancy stage compared to adult, as expected based on the high demand for

CellPress
OPEN ACCESS

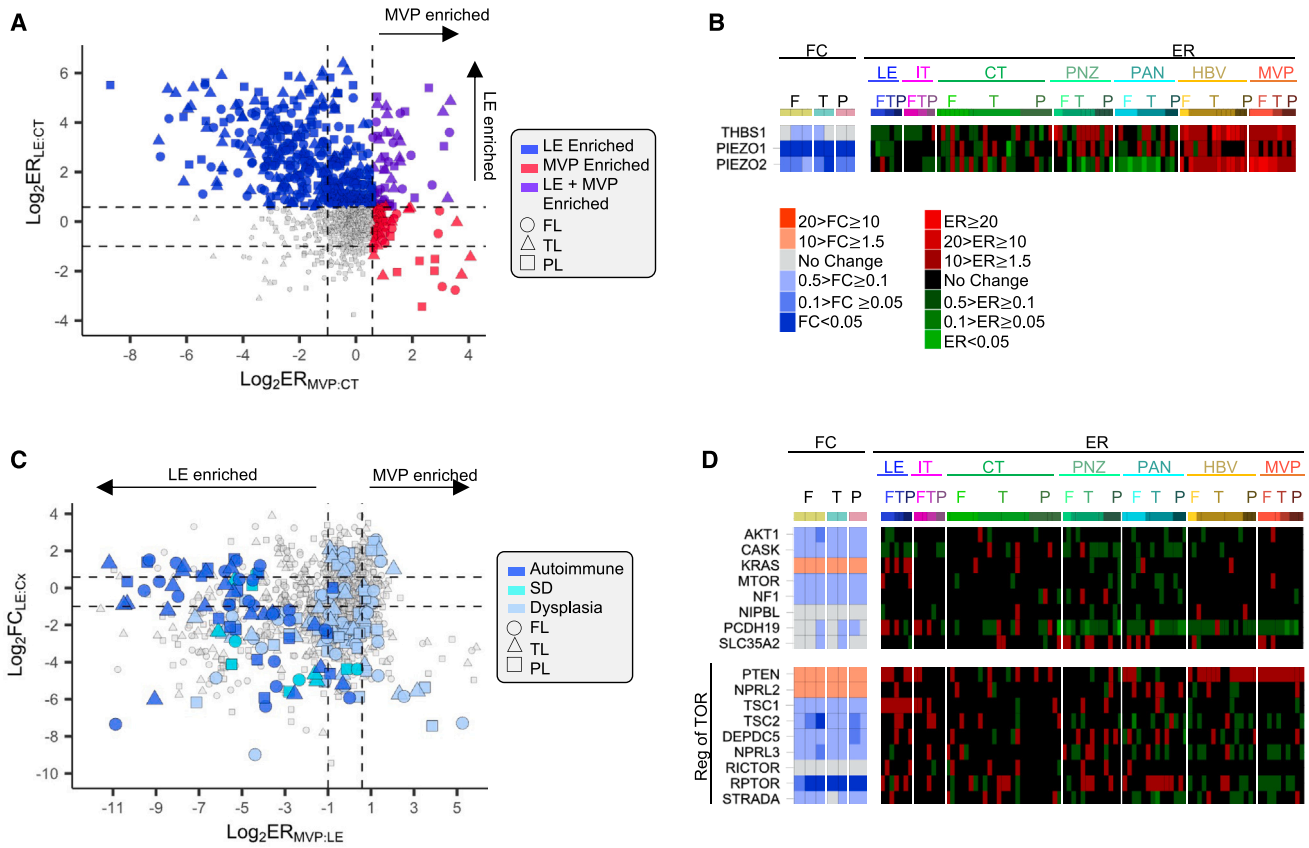

Figure 4. The LE and MVP are distinct proepileptic zones

(A) The microvasculature of proliferation is enriched in proepileptic genes. Scatterplot of the ER of the Epi358 genes for the LE and MVP regions. Based on the ER at the MVP, 32 Epi358 genes were enriched at the MVP compared to the CT, but half of these genes were also enriched at the LE.

(B) The microvasculature is enriched in potential epileptogenic genes. Heatmap of MVP-enriched genes implicated in seizures or synaptogenesis.

(C) Autoimmune epilepsy antigens are enriched at the LE but not the microvascular of proliferation zone. Scatterplot of the FC_{Cx} plotted as a function of the ER between the MVP and LE. Results show that no genes associated with autoimmune epilepsy are enriched at the MVP while nearly all of them are enriched at the LE. Genes associated with dysplasia are enriched in both the LE and MVP regions.

(D) Differences in the regulation of *MTOR* pathways at the LE and the microvascular of proliferation zone. Heatmap of the FC_{Cx} and ER of genes related to dysplasia. Growth-related genes for epileptic cortical dysplasia are dysregulated at the LE. *KRAS* is enriched and upregulated only at the LE whereas *PTEN* is enriched at the LE and MVP. *NPRL2* is also upregulated at the LE but shows no enrichment as compared to the CT. Most genes involved in cortical dysplasia did not show strong regional tumor enrichment.

neuronal displacement (Figure 5B). Glioblastoma is more prevalent in older adults (>40 years of age), but many of the *MTOR* signaling genes such as *TSC1*, *DEPDC5*, *NF1*, and *NPRL2* all showed expression levels at the LE, which more closely resemble healthy earlier development as opposed to healthy levels in adult cortex (Figure 5C). Overall, the data suggest that the LE is upregulated for specific *MTOR* signaling pathways, which are normally active during healthy cortical development.

Gene Ontology analysis also identified key differences in regulation of membrane potential and postsynaptic membrane signaling at the LE as compared to healthy development (Figure 5D). Most genes in these functions are similarly downregulated. However, less coordinate upregulation is found among pre- and postsynaptic membrane genes except in the vesicular transport to synapse cluster, which shows a high similarity of genes upregulated at the LE and in healthy development (Figure 5D). Different ion channel and transmitter subtypes modulate different functions in the developing brain versus the adult brain.[82] For example, NMDA-dependent glutamate currents enhance the survival of adult neural progenitor cells but are not required for migration.[83] On the other hand, embryonic GABA and NMDA-dependent signaling is important for radial migration of hippocampal neurons,[84] whereas embryonic AMPA receptors modulate prenatal tangential migration.[85] Intriguingly, our analysis shows that all tested NMDA receptors are downregulated similarly to prenatal stages, but none of the AMPA receptor subunits show expression patterns resembling early development (Figure 5E). For example, *GRIA1*, the only AMPA receptor upregulated in the early development of the healthy cortex (Figure 5E), is downregulated at the LE (Figure 3A). Conversely, *GRIA2*, the only AMPA receptor upregulated at the LE compared to the adult cortex (Figure 3A), is considerably downregulated at all tested developmental stages (Figure 5E). *In vitro* studies of 10–15 DIV neuronal cultures show that both NMDA and AMPA receptors

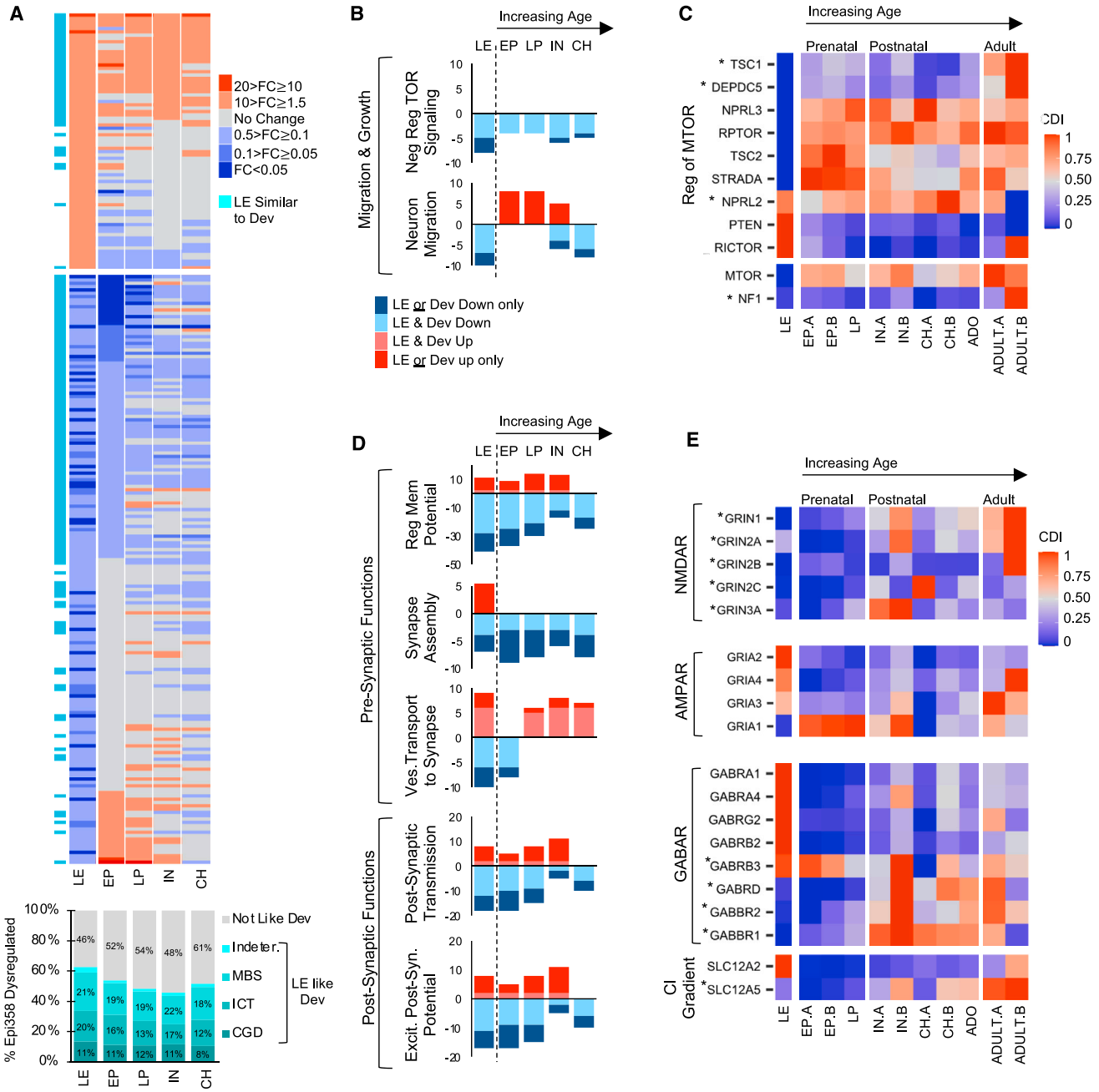

Figure 5. Peritumoral remodeling partially recapitulates early developmental programs

(A) A majority of dysregulated Epi358 genes recapitulates expression patterns in early development. Top: heatmap of the 254 dysregulated Epi358 genes (177/354 downregulated, 77/358 upregulated) and the fold change at the LE and multiple developmental stages (EP, LP, IN, CH) compared to healthy adult cortex. Genes where fold change at the LE resembles any of the tested developmental stages are marked by a cyan bar (left most column). Bottom: bar plot of the percent of dysregulated genes which resemble development (shades of cyan) stratified by the percent of genes from each functional cluster, MBS, ICT, and CGD.

(B) Recapitulation of early developmental TOR signaling at the LE. Bar plot of genes significantly enriched per growth/migration-related Gene Ontology biological process. Positive y axis represents the number of genes upregulated and negative y axis represents genes downregulated.

(C) A subset of regulators of *MTOR* signaling resembles early developmental patterns. Heatmap of the cortical developmental indices for *MTOR* signaling genes. The genes in FL glioblastoma tumor and healthy FL per developmental stage were normalized using a cortical developmental index (CDI, see Methods), revealing trends in developmental expression. Asterisks (*) denote *MTOR*-related genes, which had LE expression similar to prenatal levels.

(legend continued on next page)

can induce calcium ion influx into cells[86] and might be the source of slow inward calcium currents seen in glioma co-culture assays. However, only AMPA receptor antagonists inhibit these slow inward calcium currents *in vitro*.[50] Thus, our analysis suggests a predominant AMPA receptor-mediated slow calcium current in peritumoral networks. In contrast to the age-specific pattern seen in glutamate receptors, about half of the GABA receptor subunits resemble an early developmental stage while the other half more closely resembled adult expression levels. In healthy neocortex, the impact of GABA receptor signaling on proliferation is mixed; these receptors limit proliferation of radial glial type adult neural progenitor cells[87] but promote proliferation of a subset of type II adult neural progenitor cells with a higher internal chloride ion concentration.[88] Our analysis shows a marked decrease in *SLC12A5* (*KCC2*) at the LE (Figure 3A), but no compensatory reduction in *SLC12A2* (*NKCC1*), suggesting a higher internal chloride ion concentration resembling type II adult neural precursor cells. Thus, at the LE, *SLC12A5* levels resemble early development, but *SLC12A2* more closely resembles adult levels, which may suggest that transcriptional dysregulation at the LE suppresses *SLC12A5* expression independent of *SLC12A2* (Figure 5E). Overall, our data suggest peritumoral remodeling of a subset of genes involved in ion homeostasis resembles early development, highlighting the importance of viewing tumor-induced transcription profiles through the lens of developmental programs and mechanisms.

DISCUSSION

Spatial analysis of RNA enrichment and dysregulation patterns of genes linked to monogenic epilepsy phenotypes reveals an unexpectedly complex molecular substrate for the emergence of epistatic gene interactions in the glioblastoma cortical microenvironment. A majority of clinically validated, proepileptic gene pathways are strongly dysregulated at the tumor LE, identifying a priority gene set underlying proepileptic and antiepileptic circuit remodeling. Both gain and loss of expression in these genes, each known to critically control the balance of network excitability, define a rich network excitability dysregulome that can modify seizure risk in patients with glioblastoma. This epistatic complexity replicates the one previously reported for patterns of genomic ion channel variants in non-tumor human epilepsy cases, where computational modeling validated their combinatorial pathogenic effects.[29] The extent of epilepsy-linked transcript remodeling therefore provides a parsimonious explanation for epilepsy risk in individuals with this brain tumor, as well as a molecular basis for their pharmacoresistance to narrowly targeted conventional antiseizure medicines. A better understanding of epilepsy gene landscape patterns could identify potential targets and help guide future antiepileptic therapy for glioblastoma. For example, none of the greater than 30 currently approved antiseizure drugs target proepileptic GPCRs,[89] which are prominently upregulated at the LE.

The spatial arrangement of molecular plasticity is also informative. Unlike the "surround inhibition" motif characteristic of an acute convulsant-induced cortical seizure focus,[90] we find that tumor-induced epileptogenesis, which evolves over weeks in glioblastoma mouse models,[5] replaces this native inhibitory barrier with surround excitation. Heterogeneous profiles identified within tumor subregions distant from the margin suggest additional distinct intratumoral excitability thresholds responsible for glioma cell depolarization as well as microvascular BBB defects that could guide future clinical diagnostic classification and management. We identified striking subtype-specific changes in glutamate receptors at the tumor margin and within the tumor, for example, the strong upregulation of AMPA receptor subunits that resemble the complex cortical layer-specific changes in temporal lobe epilepsy tissue.[91] We also identify candidate BBB defects enriched at the MVP. These highly concordant patterns are masked in bulk tissue samples,[92] highlighting the value of regional analysis of malignant peritumoral networks.

The transcriptional control mechanisms driving the striking heterogeneity of epilepsy gene dysregulation within regional tumor excitability niches remain to be explored. Some genes dysregulate only in the LE, some in both the LE and tumor, and other compartmental patterns are evident. Whereas voltage-gated sodium and calcium gene dysregulation is LE predominant, enrichment of potassium channels and glutamate receptors extends into the pure tumor zone, a region largely devoid of recurrent excitatory synaptic connections critical for seizure generation, where they may nonetheless contribute to paracrine signaling affecting glial, immune, and tumor cell biology. This source of non-synaptic depolarization defines an alternative driver of tumor progression independent of EEG-detectable seizure activity. Extracellular potassium and glutamate excess in both compartments may also combine to trigger SD waves identified in mouse glioblastoma models.[5,7] These spatial excitability profiles may also refine glioblastoma subtype classification. Isocitrate dehydrogenase (*IDH*) genes are currently the primary classifiers of diffuse glioma subtypes, and their role in hyperexcitability could overlap with many metabolically linked epilepsy genes.[13] *IDH* mutation status alters normal oxidation of isocitrate to alpha-ketoglutarate in mitochondria and affects oncogenesis. In Ivy GAP, *IDH1* but not *IDH2* expression is low at the LE; both genes are markedly elevated in the tumor zone, and *IDH2* is also elevated at the MVP. Interestingly, *IDH3a* is a recent candidate risk gene for epilepsy.[93,94]

Limitations of the study

A principal limitation to interpreting the pathological transcriptome is the unclear relationship between transcript density, proteome

(D) Pre- and postsynaptic genes showed subtype-specific changes at the LE compared to normal development. Bar plot of genes significantly enriched according to their related Gene Ontology biological process. Positive y axis represents the number of genes upregulated and negative y axis represents downregulated genes.

(E) NMDA receptors and a subset of GABA receptors recapitulate early developmental patterns. Heatmap of the cortical developmental indices for major glutamate and GABA receptor genes. The genes in FL glioblastoma tumor and healthy FL samples per developmental stage were normalized using a cortical developmental index (CDI, see Methods), revealing subtype-specific trends in developmental expression. Asterisks (*) denote genes with LE levels resembling prenatal levels.

lifespan, and the plasticity of intrinsic membrane and synaptic network firing properties, each of which varies in the brain across multiple timescales. Both glioblastoma[95] and healthy neurons[96] display activity-driven circadian fluctuations in mRNA transcripts, which, once alternatively spliced, may be toxic at some synapses and imperceptible at others, and the levels themselves offer little insight into the extent of cell type-specific posttranslational modifications that could mask their final impact. For example, migrating glioblasts remodel more extensively than stationary tumor cells,[97] and both episodic seizures[98,99] and persistent depolarization[100] alter these patterns, rendering the layers of neuron-tumor crosstalk difficult to unravel. Further ambiguity resides in the potential for malignant stem cell subclones to produce multiple non-uniform lineages, as shown by discordant regional case profiles, and the age of their progeny may extend unevenly across tumor regions.[18,101,102] Therefore, even an anatomically segmented transcriptome environment is challenging to summarize across space and time and is only a molecular protomap of network hyperexcitability. Despite these limitations, as a snapshot of malignant brain tumor biology, this spatial portrait of excitability dyshomeostasis provides an invaluable reference point and a rich source of candidate gene targets for therapeutic exploration aimed at returning the peritumoral cortical landscape to its native excitability.

STAR★METHODS

Detailed methods are provided in the online version of this paper and include the following:

- KEY RESOURCES TABLE
- RESOURCES AVAILABILITY
  - Lead contact
  - Materials availability
  - Data and code availability
- EXPERIMENTAL MODEL AND SUBJECT DETAILS
- METHOD DETAILS
  - Cellular compartmentation and case complexity
  - Calculation of enrichment ratio per tumor region
  - Calculation of case concordance
  - Hierarchal clustering of the Epi358 genes into functional groups based on biological process
  - Calculation of fold change of epilepsy genes at the peritumoral LE vs. healthy cortex
  - Identification of pathogenic copy number variants that are epilepsy linked
  - Curation of gene set of disease-linked genes and presynaptic genes
  - Comparison of FC_{Cx} at the LE to expression levels during healthy early development
  - Overrepresentation analysis of development related functions
  - Determination of cortical developmental index for fold changes compared to WT
- QUANTIFICATION AND STATISTICAL ANALYSIS

SUPPLEMENTAL INFORMATION

Supplemental information can be found online at https://doi.org/10.1016/j.xcrm.2024.101691.

ACKNOWLEDGMENTS

This work was supported by NIH/NCI R01CA223388 and the Blue Bird Circle Foundation (J.L.N.).

AUTHOR CONTRIBUTIONS

J.L.N., V.S., and R.B.P. contributed to the project conceptualization and discussed results, analytical methods, and control databases. V.S. performed formal data analysis and prepared data for visualization. J.L.N. and V.S. wrote and edited the manuscript with support from R.B.P.

DECLARATION OF INTERESTS

The authors declare no competing interests.

Received: March 30, 2024
Revised: May 30, 2024
Accepted: July 25, 2024
Published: August 20, 2024

REFERENCES

1. Vecht, C., Royer-Perron, L., Houillier, C., and Huberfeld, G. (2017). Seizures and Anticonvulsants in Brain Tumours: Frequency, Mechanisms and Anti-Epileptic Management. Curr. Pharm. Des. *23*, 6464–6487. https://doi.org/10.2174/1381612823666171027130003.
2. Mastall, M., Wolpert, F., Gramatzki, D., Imbach, L., Becker, D., Schmick, A., Hertler, C., Roth, P., Weller, M., and Wirsching, H.-G. (2021). Survival of brain tumour patients with epilepsy. Brain *144*, 3322–3327. https://doi.org/10.1093/brain/awab188.
3. Mellinghoff, I.K., Van Den Bent, M.J., Blumenthal, D.T., Touat, M., Peters, K.B., Clarke, J., Mendez, J., Yust-Katz, S., Welsh, L., Mason, W.P., et al. (2023). Vorasidenib in IDH1- or IDH2-Mutant Low-Grade Glioma. N. Engl. J. Med. *389*, 589–601. https://doi.org/10.1056/NEJMoa2304194.
4. Yu, K., Lin, C.-C.J., Hatcher, A., Lozzi, B., Kong, K., Huang-Hobbs, E., Cheng, Y.-T., Beechar, V.B., Zhu, W., Zhang, Y., et al. (2020). PIK3CA variants selectively initiate brain hyperactivity during gliomagenesis. Nature *578*, 166–171. https://doi.org/10.1038/s41586-020-1952-2.
5. Hatcher, A., Yu, K., Meyer, J., Aiba, I., Deneen, B., and Noebels, J.L. (2020). Pathogenesis of peritumoral hyperexcitability in an immunocompetent CRISPR-based glioblastoma model. J. Clin. Invest. *130*, 2286–2300. https://doi.org/10.1172/JCI133316.
6. John Lin, C.-C., Yu, K., Hatcher, A., Huang, T.-W., Lee, H.K., Carlson, J., Weston, M.C., Chen, F., Zhang, Y., Zhu, W., et al. (2017). Identification of diverse astrocyte populations and their malignant analogs. Nat. Neurosci. *20*, 396–405. https://doi.org/10.1038/nn.4493.
7. Curry, R.N., Aiba, I., Meyer, J., Lozzi, B., Ko, Y., McDonald, M.F., Rosenbaum, A., Cervantes, A., Huang-Hobbs, E., Cocito, C., et al. (2023). Glioma epileptiform activity and progression are driven by IGSF3-mediated potassium dysregulation. Neuron *111*, 682–695.e9. https://doi.org/10.1016/j.neuron.2023.01.013.
8. Meyer, J., Yu, K., Luna-Figueroa, E., Deneen, B., and Noebels, J. (2024). Glioblastoma disrupts cortical network activity at multiple spatial and temporal scales. Nat. Commun. *15*, 4503. https://doi.org/10.1038/s41467-024-48757-5.
9. Robert, S.M., Buckingham, S.C., Campbell, S.L., Robel, S., Holt, K.T., Ogunrinu-Babarinde, T., Warren, P.P., White, D.M., Reid, M.A., Eschbacher, J.M., et al. (2015). SLC7A11 expression is associated with seizures and predicts poor survival in patients with malignant glioma. Sci. Transl. Med. *7*, 289ra86. https://doi.org/10.1126/scitranslmed.aaa8103.
10. Tewari, B.P., Chaunsali, L., Campbell, S.L., Patel, D.C., Goode, A.E., and Sontheimer, H. (2018). Perineuronal nets decrease membrane capacitance of peritumoral fast spiking interneurons in a model of epilepsy. Nat. Commun. *9*, 4724. https://doi.org/10.1038/s41467-018-07113-0.
11. Yeo, A.T., Rawal, S., Delcuze, B., Christofides, A., Atayde, A., Strauss, L., Balaj, L., Rogers, V.A., Uhlmann, E.J., Varma, H., et al. (2022). Single-cell RNA sequencing reveals evolution of immune landscape during glioblastoma progression. Nat. Immunol. *23*, 971–984. https://doi.org/10.1038/s41590-022-01215-0.

12. Guerrini, R., Balestrini, S., Wirrell, E.C., and Walker, M.C. (2021). Monogenic Epilepsies: Disease Mechanisms, Clinical Phenotypes, and Targeted Therapies. Neurology *97*, 817–831. https://doi.org/10.1212/WNL.0000000000012744.

13. Tumiene, B., Ferreira, C.R., and Van Karnebeek, C.D.M. (2022). 2022 Overview of Metabolic Epilepsies. Genes *13*, 508. https://doi.org/10.3390/genes13030508.

14. Kumar, P., Lim, A., Hazirah, S.N., Chua, C.J.H., Ngoh, A., Poh, S.L., Yeo, T.H., Lim, J., Ling, S., Sutamam, N.B., et al. (2022). Single-cell transcriptomics and surface epitope detection in human brain epileptic lesions identifies pro-inflammatory signaling. Nat. Neurosci. *25*, 956–966. https://doi.org/10.1038/s41593-022-01095-5.

15. Niesen, C.E., Xu, J., Fan, X., Li, X., Wheeler, C.J., Mamelak, A.N., and Wang, C. (2013). Transcriptomic Profiling of Human Peritumoral Neocortex Tissues Revealed Genes Possibly Involved in Tumor-Induced Epilepsy. PLoS One *8*, e56077. https://doi.org/10.1371/journal.pone.0056077.

16. Kalita, O., Sporikova, Z., Hajduch, M., Megova Houdova, M., Slavkovsky, R., Hrabalek, L., Halaj, M., Klementova, Y., Dolezel, M., Drabek, J., et al. (2021). The Influence of Gene Aberrations on Survival in Resected IDH Wildtype Glioblastoma Patients: A Single-Institution Study. Curr. Oncol. *28*, 1280–1293. https://doi.org/10.3390/curroncol28020122.

17. Pollak, J., Rai, K.G., Funk, C.C., Arora, S., Lee, E., Zhu, J., Price, N.D., Paddison, P.J., Ramirez, J.-M., and Rostomily, R.C. (2017). Ion channel expression patterns in glioblastoma stem cells with functional and therapeutic implications for malignancy. PLoS One *12*, e0172884. https://doi.org/10.1371/journal.pone.0172884.

18. Neftel, C., Laffy, J., Filbin, M.G., Hara, T., Shore, M.E., Rahme, G.J., Richman, A.R., Silverbush, D., Shaw, M.L., Hebert, C.M., et al. (2019). An Integrative Model of Cellular States, Plasticity, and Genetics for Glioblastoma. Cell *178*, 835–849.e21. https://doi.org/10.1016/j.cell.2019.06.024.

19. Puchalski, R.B., Shah, N., Miller, J., Dalley, R., Nomura, S.R., Yoon, J.-G., Smith, K.A., Lankerovich, M., Bertagnolli, D., Bickley, K., et al. (2018). An anatomic transcriptional atlas of human glioblastoma. Science *360*, 660–663. https://doi.org/10.1126/science.aaf2666.

20. Kádková, A., Murach, J., Østergaard, M., Malsam, A., Malsam, J., Lolicato, F., Nickel, W., Söllner, T.H., and Sørensen, J.B. (2024). SNAP25 disease mutations change the energy landscape for synaptic exocytosis due to aberrant SNARE interactions. Elife *12*, RP88619. https://doi.org/10.7554/eLife.88619.

21. Huang, Q., Lian, C., Dong, Y., Zeng, H., Liu, B., Xu, N., He, Z., and Guo, H. (2021). SNAP25 Inhibits Glioma Progression by Regulating Synapse Plasticity via GLS-Mediated Glutaminolysis. Front. Oncol. *11*, 698835. https://doi.org/10.3389/fonc.2021.698835.

22. Chernova, O.B., Somerville, R.P., and Cowell, J.K. (1998). A novel gene, LGI1, from 10q24 is rearranged and downregulated in malignant brain tumors. Oncogene *17*, 2873–2881. https://doi.org/10.1038/sj.onc.1202481.

23. Schulte, U., Thumfart, J.-O., Klöcker, N., Sailer, C.A., Bildl, W., Biniossek, M., Dehn, D., Deller, T., Eble, S., Abbass, K., et al. (2006). The Epilepsy-Linked Lgi1 Protein Assembles into Presynaptic Kv1 Channels and Inhibits Inactivation by Kvβ1. Neuron *49*, 697–706. https://doi.org/10.1016/j.neuron.2006.01.033.

24. Nobile, C., Michelucci, R., Andreazza, S., Pasini, E., Tosatto, S.C.E., and Striano, P. (2009). *LGI1* mutations in autosomal dominant and sporadic lateral temporal epilepsy. Hum. Mutat. *30*, 530–536. https://doi.org/10.1002/humu.20925.

25. Uhlén, M., Fagerberg, L., Hallström, B.M., Lindskog, C., Oksvold, P., Mardinoglu, A., Sivertsson, Å., Kampf, C., Sjöstedt, E., Asplund, A., et al. (2015). Tissue-based map of the human proteome. Science *347*, 1260419. https://doi.org/10.1126/science.1260419.

26. Carvill, G.L., Matheny, T., Hesselberth, J., and Demarest, S. (2021). Haploinsufficiency, Dominant Negative, and Gain-of-Function Mechanisms in Epilepsy: Matching Therapeutic Approach to the Pathophysiology. Neurotherapeutics *18*, 1500–1514. https://doi.org/10.1007/s13311-021-01137-z.

27. Brünger, T., Pérez-Palma, E., Montanucci, L., Nothnagel, M., Møller, R.S., Schorge, S., Zuberi, S., Symonds, J., Lemke, J.R., Brunklaus, A., et al. (2023). Conserved patterns across ion channels correlate with variant pathogenicity and clinical phenotypes. Brain *146*, 923–934. https://doi.org/10.1093/brain/awac305.

28. Glasscock, E., Qian, J., Yoo, J.W., and Noebels, J.L. (2007). Masking epilepsy by combining two epilepsy genes. Nat. Neurosci. *10*, 1554–1558. https://doi.org/10.1038/nn1999.

29. Klassen, T., Davis, C., Goldman, A., Burgess, D., Chen, T., Wheeler, D., McPherson, J., Bourquin, T., Lewis, L., Villasana, D., et al. (2011). Exome Sequencing of Ion Channel Genes Reveals Complex Profiles Confounding Personal Risk Assessment in Epilepsy. Cell *145*, 1036–1048. https://doi.org/10.1016/j.cell.2011.05.025.

30. Conti, L., Crisafulli, L., Caldera, V., Tortoreto, M., Brilli, E., Conforti, P., Zunino, F., Magrassi, L., Schiffer, D., and Cattaneo, E. (2012). REST Controls Self-Renewal and Tumorigenic Competence of Human Glioblastoma Cells. PLoS One *7*, e38486. https://doi.org/10.1371/journal.pone.0038486.

31. Krishna, S., Choudhury, A., Keough, M.B., Seo, K., Ni, L., Kakaizada, S., Lee, A., Aabedi, A., Popova, G., Lipkin, B., et al. (2023). Glioblastoma remodelling of human neural circuits decreases survival. Nature *617*, 599–607. https://doi.org/10.1038/s41586-023-06036-1.

32. Mayo, S., Gómez-Manjón, I., Marco-Hernández, A.V., Fernández-Martínez, F.J., Camacho, A., and Martínez, F. (2023). N-Type Ca Channel in Epileptic Syndromes and Epilepsy: A Systematic Review of Its Genetic Variants. Int. J. Mol. Sci. *24*, 6100. https://doi.org/10.3390/ijms24076100.

33. Ernst, W.L., Zhang, Y., Yoo, J.W., Ernst, S.J., and Noebels, J.L. (2009). Genetic Enhancement of Thalamocortical Network Activity by Elevating α1G-Mediated Low-Voltage-Activated Calcium Current Induces Pure Absence Epilepsy. J. Neurosci. *29*, 1615–1625. https://doi.org/10.1523/JNEUROSCI.2081-08.2009.

34. Song, I., Kim, D., Choi, S., Sun, M., Kim, Y., and Shin, H.-S. (2004). Role of the α1G T-Type Calcium Channel in Spontaneous Absence Seizures in Mutant Mice. J. Neurosci. *24*, 5249–5257. https://doi.org/10.1523/JNEUROSCI.5546-03.2004.

35. D'Adamo, M.C., Catacuzzeno, L., Di Giovanni, G., Franciolini, F., and Pessia, M. (2013). K+ channelepsy: progress in the neurobiology of potassium channels and epilepsy. Front. Cell. Neurosci. *7*, 134. https://doi.org/10.3389/fncel.2013.00134.

36. Niday, Z., and Tzingounis, A.V. (2018). Potassium Channel Gain of Function in Epilepsy: An Unresolved Paradox. Neuroscientist *24*, 368–380. https://doi.org/10.1177/1073858418763752.

37. Trimmer, J.S. (2015). Subcellular Localization of K+ Channels in Mammalian Brain Neurons: Remarkable Precision in the Midst of Extraordinary Complexity. Neuron *85*, 238–256. https://doi.org/10.1016/j.neuron.2014.12.042.

38. Cuddapah, V.A., Turner, K.L., Seifert, S., and Sontheimer, H. (2013). Bradykinin-Induced Chemotaxis of Human Gliomas Requires the Activation of K_{Ca} 3.1 and ClC-3. J. Neurosci. *33*, 1427–1440. https://doi.org/10.1523/JNEUROSCI.3980-12.2013.

39. Prevarskaya, N., Skryma, R., and Shuba, Y. (2018). Ion Channels in Cancer: Are Cancer Hallmarks Oncochannelopathies? Physiol. Rev. *98*, 559–621. https://doi.org/10.1152/physrev.00044.2016.

40. Petersson, S., Persson, A.-S., Johansen, J.E., Ingvar, M., Nilsson, J., Klement, G., Arhem, P., Schalling, M., and Lavebratt, C. (2003). Truncation of the Shaker-like voltage-gated potassium channel, Kv1.1, causes megencephaly. Eur. J. Neurosci. *18*, 3231–3240. https://doi.org/10.1111/j.1460-9568.2003.03044.x.

41. Hills, K.E., Kostarelos, K., and Wykes, R.C. (2022). Converging Mechanisms of Epileptogenesis and Their Insight in Glioblastoma. Front. Mol. Neurosci. *15*, 903115. https://doi.org/10.3389/fnmol.2022.903115.

42. Eikermann-Haerter, K., Yuzawa, I., Qin, T., Wang, Y., Baek, K., Kim, Y.R., Hoffmann, U., Dilekoz, E., Waeber, C., Ferrari, M.D., et al. (2011). Enhanced Subcortical Spreading Depression in Familial Hemiplegic Migraine Type 1 Mutant Mice. J. Neurosci. *31*, 5755–5763. https://doi.org/10.1523/JNEUROSCI.5346-10.2011.

43. Reiffurth, C., Alam, M., Zahedi-Khorasani, M., Major, S., and Dreier, J.P. (2020). Na $^{+}$/K $^{+}$ -ATPase α isoform deficiency results in distinct spreading depolarization phenotypes. J. Cereb. Blood Flow Metab. *40*, 622–638. https://doi.org/10.1177/0271678X19833757.

44. Aiba, I., Ning, Y., and Noebels, J.L. (2023). A hyperthermic seizure unleashes a surge of spreading depolarizations in Scn1a-deficient mice. JCI Insight *8*, e170399. https://doi.org/10.1172/jci.insight.170399.

45. Kessi, M., Peng, J., Duan, H., He, H., Chen, B., Xiong, J., Wang, Y., Yang, L., Wang, G., Kiprotich, K., et al. (2022). The Contribution of HCN Channelopathies in Different Epileptic Syndromes, Mechanisms, Modulators, and Potential Treatment Targets: A Systematic Review. Front. Mol. Neurosci. *15*, 807202. https://doi.org/10.3389/fnmol.2022.807202.

46. Faragó, N., Kocsis, Á.K., Braskó, C., Lovas, S., Rózsa, M., Baka, J., Kovács, B., Mikite, K., Szemenyei, V., Molnár, G., et al. (2016). Human neuronal changes in brain edema and increased intracranial pressure. Acta Neuropathol. Commun. *4*, 78. https://doi.org/10.1186/s40478-016-0356-x.

47. Nakamura, Y., Inoue, A., Nishikawa, M., Ohnishi, T., Yano, H., Kanemura, Y., Ohtsuka, Y., Ozaki, S., Kusakabe, K., Suehiro, S., et al. (2022). Quantitative measurement of peritumoral concentrations of glutamate, N-acetyl aspartate, and lactate on magnetic resonance spectroscopy predicts glioblastoma-related refractory epilepsy. Acta Neurochir. *164*, 3253–3266. https://doi.org/10.1007/s00701-022-05363-y.

48. Buckingham, S.C., Campbell, S.L., Haas, B.R., Montana, V., Robel, S., Ogunrinu, T., and Sontheimer, H. (2011). Glutamate release by primary brain tumors induces epileptic activity. Nat. Med. *17*, 1269–1274. https://doi.org/10.1038/nm.2453.

49. Takano, T., Lin, J.H., Arcuino, G., Gao, Q., Yang, J., and Nedergaard, M. (2001). Glutamate release promotes growth of malignant gliomas. Nat. Med. *7*, 1010–1015. https://doi.org/10.1038/nm0901-1010.

50. Venkataramani, V., Tanev, D.I., Strahle, C., Studier-Fischer, A., Fankhauser, L., Kessler, T., Körber, C., Kardorff, M., Ratliff, M., Xie, R., et al. (2019). Glutamatergic synaptic input to glioma cells drives brain tumour progression. Nature *573*, 532–538. https://doi.org/10.1038/s41586-019-1564-x.

51. Tardito, S., Oudin, A., Ahmed, S.U., Fack, F., Keunen, O., Zheng, L., Miletic, H., Sakariassen, P.Ø., Weinstock, A., Wagner, A., et al. (2015). Glutamine synthetase activity fuels nucleotide biosynthesis and supports growth of glutamine-restricted glioblastoma. Nat. Cell Biol. *17*, 1556–1568. https://doi.org/10.1038/ncb3272.

52. Ye, Z.-C., Rothstein, J.D., and Sontheimer, H. (1999). Compromised Glutamate Transport in Human Glioma Cells: Reduction–Mislocalization of Sodium-Dependent Glutamate Transporters and Enhanced Activity of Cystine–Glutamate Exchange. J. Neurosci. *19*, 10767–10777. https://doi.org/10.1523/JNEUROSCI.19-24-10767.1999.

53. Ishiuchi, S., Yoshida, Y., Sugawara, K., Aihara, M., Ohtani, T., Watanabe, T., Saito, N., Tsuzuki, K., Okado, H., Miwa, A., et al. (2007). Ca^{2+} -Permeable AMPA Receptors Regulate Growth of Human Glioblastoma via Akt Activation. J. Neurosci. *27*, 7987–8001. https://doi.org/10.1523/JNEUROSCI.2180-07.2007.

54. Taylor, K.R., Barron, T., Hui, A., Spitzer, A., Yalçin, B., Ivec, A.E., Geraghty, A.C., Hartmann, G.G., Arzt, M., Gillespie, S.M., et al. (2023). Glioma synapses recruit mechanisms of adaptive plasticity. Nature *623*, 366–374. https://doi.org/10.1038/s41586-023-06678-1.

55. Chatron, N., Becker, F., Morsy, H., Schmidts, M., Hardies, K., Tuysuz, B., Roselli, S., Najafi, M., Alkaya, D.U., Ashrafzadeh, F., et al. (2020). Biallelic GAD1 variants cause a neonatal onset syndromic developmental and epileptic encephalopathy. Brain *143*, 1447–1461. https://doi.org/10.1093/brain/awaa085.

56. Kash, S.F., Johnson, R.S., Tecott, L.H., Noebels, J.L., Mayfield, R.D., Hanahan, D., and Baekkeskov, S. (1997). Epilepsy in mice deficient in the 65-kDa isoform of glutamic acid decarboxylase. Proc. Natl. Acad. Sci. USA *94*, 14060–14065. https://doi.org/10.1073/pnas.94.25.14060.

57. Klitten, L.L., Møller, R.S., Ravn, K., Hjalgrim, H., and Tommerup, N. (2011). Duplication of MAOA, MAOB, and NDP in a patient with mental retardation and epilepsy. Eur. J. Hum. Genet. *19*, 1–2. https://doi.org/10.1038/ejhg.2010.149.

58. Maillard, P.Y., Baer, S., Schaefer, É., Desnous, B., Villeneuve, N., Lépine, A., Fabre, A., Lacoste, C., El Chehadeh, S., Piton, A., et al. (2022). Molecular and clinical descriptions of patients with GABA $_A$ receptor gene variants (*GABRA1*, *GABRB2*, *GABRB3*, *GABRG2*): A cohort study, review of literature, and genotype–phenotype correlation. Epilepsia *63*, 2519–2533. https://doi.org/10.1111/epi.17336.

59. Dossi, E., and Huberfeld, G. (2023). GABAergic circuits drive focal seizures. Neurobiol. Dis. *180*, 106102. https://doi.org/10.1016/j.nbd.2023.106102.

60. Tian, J., Chau, C., Hales, T.G., and Kaufman, D.L. (1999). GABAA receptors mediate inhibition of T cell responses. J. Neuroimmunol. *96*, 21–28. https://doi.org/10.1016/S0165-5728(98)00264-1.

61. Blanchart, A., Fernando, R., Häring, M., Assaife-Lopes, N., Romanov, R.A., Andäng, M., Harkany, T., and Ernfors, P. (2017). Endogenous GABAA receptor activity suppresses glioma growth. Oncogene *36*, 777–786. https://doi.org/10.1038/onc.2016.245.

62. Smits, A., Jin, Z., Elsir, T., Pedder, H., Nistér, M., Alafuzoff, I., Dimberg, A., Edqvist, P.-H., Pontén, F., Aronica, E., and Birnir, B. (2012). GABA-A Channel Subunit Expression in Human Glioma Correlates with Tumor Histology and Clinical Outcome. PLoS One *7*, e37041. https://doi.org/10.1371/journal.pone.0037041.

63. Levinson, S., Tran, C.H., Barry, J., Viker, B., Levine, M.S., Vinters, H.V., Mathern, G.W., and Cepeda, C. (2020). Paroxysmal Discharges in Tissue Slices From Pediatric Epilepsy Surgery Patients: Critical Role of GABAB Receptors in the Generation of Ictal Activity. Front. Cell. Neurosci. *14*, 54. https://doi.org/10.3389/fncel.2020.00054.

64. Duy, P.Q., David, W.B., and Kahle, K.T. (2019). Identification of KCC2 Mutations in Human Epilepsy Suggests Strategies for Therapeutic Transporter Modulation. Front. Cell. Neurosci. *13*, 515. https://doi.org/10.3389/fncel.2019.00515.

65. Moore, Y.E., Deeb, T.Z., Chadchankar, H., Brandon, N.J., and Moss, S.J. (2018). Potentiating KCC2 activity is sufficient to limit the onset and severity of seizures. Proc. Natl. Acad. Sci. USA *115*, 10166–10171. https://doi.org/10.1073/pnas.1810134115.

66. Pallud, J., Le Van Quyen, M., Bielle, F., Pellegrino, C., Varlet, P., Cresto, N., Baulac, M., Duyckaerts, C., Kourdougli, N., Chazal, G., et al. (2014). Cortical GABAergic excitation contributes to epileptic activities around human glioma. Sci. Transl. Med. *6*, 244ra89. https://doi.org/10.1126/scitranslmed.3008065.

67. Campbell, S.L., Robel, S., Cuddapah, V.A., Robert, S., Buckingham, S.C., Kahle, K.T., and Sontheimer, H. (2015). GABAergic disinhibition and impaired KCC2 cotransporter activity underlie tumor-associated epilepsy: Reduced KCC2 Underlie Tumor-Related Epilepsy. Glia *63*, 23–36. https://doi.org/10.1002/glia.22730.

68. MacKenzie, G., O'Toole, K.K., Moss, S.J., and Maguire, J. (2016). Compromised GABAergic inhibition contributes to tumor-associated epilepsy. Epilepsy Res. *126*, 185–196. https://doi.org/10.1016/j.eplepsyres.2016.07.010.

69. Montgomery, M.K., Kim, S.H., Dovas, A., Zhao, H.T., Goldberg, A.R., Xu, W., Yagielski, A.J., Cambareri, M.K., Patel, K.B., Mela, A., et al. (2020). Glioma-Induced Alterations in Neuronal Activity and Neurovascular Coupling during Disease Progression. Cell Rep. *31*, 107500. https://doi.org/10.1016/j.celrep.2020.03.064.

70. Ren, Y., Liu, Y., Wu, H., Meng, Q., Zhang, J., Li, H., Dong, S., Lian, H., Du, C., and Zhang, H. (2023). Subdural osteoma in an adolescent patient with epilepsy: an unusual case report and literature review. Childs Nerv. Syst. *39*, 3281–3288. https://doi.org/10.1007/s00381-023-06015-x.

71. Löscher, W., and Friedman, A. (2020). Structural, Molecular, and Functional Alterations of the Blood-Brain Barrier during Epileptogenesis and Epilepsy: A Cause, Consequence, or Both? Int. J. Mol. Sci. *21*, 591. https://doi.org/10.3390/ijms21020591.

72. Geis, C., Planagumà, J., Carreño, M., Graus, F., and Dalmau, J. (2019). Autoimmune seizures and epilepsy. J. Clin. Invest. *129*, 926–940. https://doi.org/10.1172/JCI125178.

73. Flammer, J., Neziraj, T., Rüegg, S., and Pröbstel, A.-K. (2023). Immune Mechanisms in Epileptogenesis: Update on Diagnosis and Treatment of Autoimmune Epilepsy Syndromes. Drugs *83*, 135–158. https://doi.org/10.1007/s40265-022-01826-9.

74. Vogrig, A., Gigli, G.L., Segatti, S., Corazza, E., Marini, A., Bernardini, A., Valent, F., Fabris, M., Curcio, F., Brigo, F., et al. (2020). Epidemiology of paraneoplastic neurological syndromes: a population-based study. J. Neurol. *267*, 26–35. https://doi.org/10.1007/s00415-019-09544-1.

75. Giammello, F., Galletta, K., Grillo, F., Brizzi, T., Cavallaro, M., Mormina, E., Scelzo, E., Allegra, C., Stancanelli, C., Rodolico, C., et al. (2023). Paraneoplastic neurological syndromes of the central nervous system: a single institution 7-year case series. Acta Neurol. *123*, 1355–1369. https://doi.org/10.1007/s13760-023-02232-y.

76. Rokutanda, T., Inatomi, Y., Yonehara, T., Takahashi, Y., Hirano, T., and Uchino, M. (2008). A case of glioblastoma misdiagnosed initially due to positive finding of anti-glutamate receptor antibody. Rinsho Shinkeigaku *48*, 497–500. https://doi.org/10.5692/clinicalneurol.48.497.

77. López-Rivera, J.A., Leu, C., Macnee, M., Khoury, J., Hoffmann, L., Coras, R., Kobow, K., Bhattarai, N., Pérez-Palma, E., Hamer, H., et al. (2023). The genomic landscape across 474 surgically accessible epileptogenic human brain lesions. Brain *146*, 1342–1356. https://doi.org/10.1093/brain/awac376.

78. Kim, J.K., Cho, J., Kim, S.H., Kang, H.-C., Kim, D.-S., Kim, V.N., and Lee, J.H. (2019). Brain somatic mutations in MTOR reveal translational dysregulations underlying intractable focal epilepsy. J. Clin. Invest. *129*, 4207–4223. https://doi.org/10.1172/JCI127032.

79. Chung, C., Yang, X., Bae, T., Vong, K.I., Mittal, S., Donkels, C., Westley Phillips, H., Li, Z., Marsh, A.P.L., Breuss, M.W., et al. (2023). Comprehensive multi-omic profiling of somatic mutations in malformations of cortical development. Nat. Genet. *55*, 209–220. https://doi.org/10.1038/s41588-022-01276-9.

80. Schreck, K.C., Allen, A.N., Wang, J., and Pratilas, C.A. (2020). Combination MEK and mTOR inhibitor therapy is active in models of glioblastoma. Neuro-Oncol. Adv *2*, vdaa138. https://doi.org/10.1093/noajnl/vdaa138.

81. Jung, E., Alfonso, J., Monyer, H., Wick, W., and Winkler, F. (2020). Neuronal signatures in cancer. Int. J. Cancer *147*, 3281–3291. https://doi.org/10.1002/ijc.33138.

82. Götz, M., Nakafuku, M., and Petrik, D. (2016). Neurogenesis in the Developing and Adult Brain-Similarities and Key Differences. Cold Spring Harb. Perspect. Biol. *8*, a018853. https://doi.org/10.1101/cshperspect.a018853.

83. Platel, J.-C., Dave, K.A., Gordon, V., Lacar, B., Rubio, M.E., and Bordey, A. (2010). NMDA receptors activated by subventricular zone astrocytic glutamate are critical for neuroblast survival prior to entering a synaptic network. Neuron *65*, 859–872. https://doi.org/10.1016/j.neuron.2010.03.009.

84. Manent, J.-B., Demarque, M., Jorquera, I., Pellegrino, C., Ben-Ari, Y., Aniksztejn, L., and Represa, A. (2005). A noncanonical release of GABA and glutamate modulates neuronal migration. J. Neurosci. *25*, 4755–4765. https://doi.org/10.1523/JNEUROSCI.0553-05.2005.

85. Manent, J.-B., Jorquera, I., Ben-Ari, Y., Aniksztejn, L., and Represa, A. (2006). Glutamate acting on AMPA but not NMDA receptors modulates the migration of hippocampal interneurons. J. Neurosci. *26*, 5901–5909. https://doi.org/10.1523/JNEUROSCI.1033-06.2006.

86. Fischer, W., Franke, H., Scheibler, P., Allgaier, C., and Illes, P. (2002). AMPA-induced Ca(2+) influx in cultured rat cortical nonpyramidal neurones: pharmacological characterization using fura-2 microfluorimetry. Eur. J. Pharmacol. *438*, 53–62. https://doi.org/10.1016/s0014-2999(02)01296-7.

87. Liu, X., Wang, Q., Haydar, T.F., and Bordey, A. (2005). Nonsynaptic GABA signaling in postnatal subventricular zone controls proliferation of GFAP-expressing progenitors. Nat. Neurosci. *8*, 1179–1187. https://doi.org/10.1038/nn1522.

88. Tozuka, Y., Fukuda, S., Namba, T., Seki, T., and Hisatsune, T. (2005). GABAergic excitation promotes neuronal differentiation in adult hippocampal progenitor cells. Neuron *47*, 803–815. https://doi.org/10.1016/j.neuron.2005.08.023.

89. Yu, Y., Nguyen, D.T., and Jiang, J. (2019). G protein-coupled receptors in acquired epilepsy: Druggability and translatability. Prog. Neurobiol. *183*, 101682. https://doi.org/10.1016/j.pneurobio.2019.101682.

90. Prince, D.A., and Wilder, B.J. (1967). Control Mechanisms in Cortical Epileptogenic Foci*: "Surround" Inhibition. Arch. Neurol. *16*, 194–202. https://doi.org/10.1001/archneur.1967.00470200082007.

91. Pfisterer, U., Petukhov, V., Demharter, S., Meichsner, J., Thompson, J.J., Batiuk, M.Y., Asenjo-Martinez, A., Vasistha, N.A., Thakur, A., Mikkelsen, J., et al. (2020). Identification of epilepsy-associated neuronal subtypes and gene expression underlying epileptogenesis. Nat. Commun. *11*, 5038. https://doi.org/10.1038/s41467-020-18752-7.

92. Elias, A.F., Lin, B.C., and Piggott, B.J. (2023). Ion Channels in Gliomas—From Molecular Basis to Treatment. Int. J. Mol. Sci. *24*, 2530. https://doi.org/10.3390/ijms24032530.

93. Drumm, M.R., Wang, W., Sears, T.K., Bell-Burdett, K., Javier, R., Cotton, K.Y., Webb, B., Byrne, K., Unruh, D., Thirunavu, V., et al. (2023). Postoperative risk of IDH mutant glioma–associated seizures and their potential management with IDH mutant inhibitors. J. Clin. Invest. *133*, e168035. https://doi.org/10.1172/JCI168035.

94. Van Opijnen, M.P., Tesileanu, C.M.S., Dirven, L., Van Der Meer, P.B., Wijnenga, M.M.J., Vincent, A.J.P.E., Broekman, M.L.D., Dubbink, H.J., Kros, J.M., Van Duinen, S.G., et al. (2023). *IDH1/2* wildtype gliomas grade 2 and 3 with molecular glioblastoma-like profile have a distinct course of epilepsy compared to *IDH1/2* wildtype glioblastomas. Neuro Oncol. *25*, 701–709. https://doi.org/10.1093/neuonc/noac197.

95. Dong, Z., Zhang, G., Qu, M., Gimple, R.C., Wu, Q., Qiu, Z., Prager, B.C., Wang, X., Kim, L.J.Y., Morton, A.R., et al. (2019). Targeting Glioblastoma Stem Cells through Disruption of the Circadian Clock. Cancer Discov. *9*, 1556–1573. https://doi.org/10.1158/2159-8290.CD-19-0215.

96. Gonzalez, J.C., Lee, H., Vincent, A.M., Hill, A.L., Goode, L.K., King, G.D., Gamble, K.L., Wadiche, J.I., and Overstreet-Wadiche, L. (2023). Circadian regulation of dentate gyrus excitability mediated by G-protein signaling. Cell Rep. *42*, 112039. https://doi.org/10.1016/j.celrep.2023.112039.

97. Cuddapah, V.A., Robel, S., Watkins, S., and Sontheimer, H. (2014). A neurocentric perspective on glioma invasion. Nat. Rev. Neurosci. *15*, 455–465. https://doi.org/10.1038/nrn3765.

98. Berger, T.C., Vigeland, M.D., Hjorthaug, H.S., Etholm, L., Nome, C.G., Taubøll, E., Heuser, K., and Selmer, K.K. (2019). Neuronal and glial DNA methylation and gene expression changes in early epileptogenesis. PLoS One *14*, e0226575. https://doi.org/10.1371/journal.pone.0226575.

99. Soon, H.R., Gaunt, J.R., Bansal, V.A., Lenherr, C., Sze, S.K., and Ch'ng, T.H. (2023). Seizure enhances SUMOylation and zinc-finger transcriptional repression in neuronal nuclei. iScience *26*, 107707. https://doi.org/10.1016/j.isci.2023.107707.

100. Xu, X., Johnson, Z., and Xie, H. (2022). Neuronal Depolarization Induced RNA m5C Methylation Changes in Mouse Cortical Neurons. Biology *11*, 988. https://doi.org/10.3390/biology11070988.

101. Tirosh, I., and Suvà, M.L. (2020). Tackling the Many Facets of Glioblastoma Heterogeneity. Cell Stem Cell *26*, 303–304. https://doi.org/10.1016/j.stem.2020.02.005.

102. Couturier, C.P., Ayyadhury, S., Le, P.U., Nadaf, J., Monlong, J., Riva, G., Allache, R., Baig, S., Yan, X., Bourgey, M., et al. (2020). Single-cell RNA-seq reveals that glioblastoma recapitulates a normal neurodevelopmental hierarchy. Nat. Commun. *11*, 3406. https://doi.org/10.1038/s41467-020-17186-5.

103. Schaff, L.R., and Mellinghoff, I.K. (2023). Glioblastoma and Other Primary Brain Malignancies in Adults: A Review. JAMA *329*, 574–587. https://doi.org/10.1001/jama.2023.0023.

104. Yu, G., Li, F., Qin, Y., Bo, X., Wu, Y., and Wang, S. (2010). GOSemSim: an R package for measuring semantic similarity among GO terms and gene products. Bioinforma. Oxf. Engl. *26*, 976–978. https://doi.org/10.1093/bioinformatics/btq064.

105. Boyle, E.I., Weng, S., Gollub, J., Jin, H., Botstein, D., Cherry, J.M., and Sherlock, G. (2004). GO::TermFinder–open source software for accessing Gene Ontology information and finding significantly enriched Gene Ontology terms associated with a list of genes. Bioinforma. Oxf. Engl. *20*, 3710–3715. https://doi.org/10.1093/bioinformatics/bth456.

106. Wu, T., Hu, E., Xu, S., Chen, M., Guo, P., Dai, Z., Feng, T., Zhou, L., Tang, W., Zhan, L., et al. (2021). clusterProfiler 4.0: A universal enrichment tool for interpreting omics data. Innovation *2*, 100141. https://doi.org/10.1016/j.xinn.2021.100141.

107. Xu, S., Dai, Z., Guo, P., Fu, X., Liu, S., Zhou, L., Tang, W., Feng, T., Chen, M., Zhan, L., et al. (2021). ggtreeExtra: Compact Visualization of Richly Annotated Phylogenetic Data. Mol. Biol. Evol. *38*, 4039–4042. https://doi.org/10.1093/molbev/msab166.

108. Miller, J.A., Ding, S.-L., Sunkin, S.M., Smith, K.A., Ng, L., Szafer, A., Ebbert, A., Riley, Z.L., Royall, J.J., Aiona, K., et al. (2014). Transcriptional landscape of the prenatal human brain. Nature *508*, 199–206. https://doi.org/10.1038/nature13185.

109. Collins, R.L., Glessner, J.T., Porcu, E., Lepamets, M., Brandon, R., Lauricella, C., Han, L., Morley, T., Niestroj, L.-M., Ulirsch, J., et al. (2022). A cross-disorder dosage sensitivity map of the human genome. Cell *185*, 3041–3055.e25. https://doi.org/10.1016/j.cell.2022.06.036.

110. Gandal, M.J., Nesbitt, A.M., McCurdy, R.M., and Alter, M.D. (2012). Measuring the maturity of the fast-spiking interneuron transcriptional program in autism, schizophrenia, and bipolar disorder. PLoS One *7*, e41215. https://doi.org/10.1371/journal.pone.0041215.

111. Hanamsagar, R., Alter, M.D., Block, C.S., Sullivan, H., Bolton, J.L., and Bilbo, S.D. (2017). Generation of a microglial developmental index in mice and in humans reveals a sex difference in maturation and immune reactivity. Glia *65*, 1504–1520. https://doi.org/10.1002/glia.23176.

STAR★METHODS

KEY RESOURCES TABLE

REAGENT or RESOURCE	SOURCE	IDENTIFIER
Deposited data		
Ivy GAP	Allen Brain Institute	https://glioblastoma.alleninstitute.org/rnaseq/search/index.html
RNA TCGA cancer sample gene data, Human Protein Atlas version 23.0, Ensembl version 109	Human Protein Atlas	https://www.proteinatlas.org/about/download
BrainSpan	Allen Brain Institute	https://www.brainspan.org/
RNA HPA brain gene data, The Human Protein Atlas version 23.0 and Ensembl version 109	Human Protein Atlas	https://www.proteinatlas.org/about/download
RNA HPA PFC brain gene data, The Human Protein Atlas version 23.0 and Ensembl version 109.	Human Protein Atlas	https://www.proteinatlas.org/about/download
Software and algorithms		
ggplot2	R	https://cran.r-project.org/web/packages/ggplot2/index.html
Tidyverse	R	https://cran.r-project.org/web/packages/tidyverse/index.html
clusterProfiler	Bioconductor	https://bioconductor.org/packages/release/bioc/html/clusterProfiler.html
GOSemSims	Bioconductor	https://bioconductor.org/packages/release/bioc/html/GOSemSim.html
STAT	R	https://cran.r-project.org/web/packages/STAT/index.html
tidytree	R	https://cran.r-project.org/web/packages/tidytree/index.html
ggtreeExtra	Bioconductor	https://bioconductor.org/packages/release/bioc/html/ggtreeExtra.html

RESOURCES AVAILABILITY

Lead contact

Further information and requests for resources and reagents should be directed to and will be fulfilled by the lead contact, Jeffrey Noebels (jnoebels@bcm.edu).

Materials availability

This study did not generate any new reagents.

Data and code availability

Data used in this study are listed in the key resource table and are detailed in the Methods Details section below. No original code was generated for this study. All heatmaps were generated using *ggplot2* and *Tidyverse* packages in R. Any additional information required to reanalyze the data reported in this work is available from the lead contact upon request.

EXPERIMENTAL MODEL AND SUBJECT DETAILS

This study did not generate any new experimental models. Information about cases analyzed in this study are listed in references detailed in the Methods Details section.

METHOD DETAILS

Cellular compartmentation and case complexity

The Ivy GAP[19] database was generated by microscopically sampling 7 resected tumor regions, including the neuronal leading edge (LE) and adjacent zones of infiltrating tumor (IT), dense tumor cells (CT), perinecrotic zone (PNZ), pseudopalisading necrosis (PAN),

hyperplastic blood vessel in the cellular tumor (HBV) and microvascular proliferation (MVP). Each region was identified histologically and validated with cell-type specific RNA-Seq population markers.

Histological definitions of tumor regions

The leading edge (LE) samples were selected to contain zones containing only 1–3 tumor cells per visual field reflecting peritumoral neural networks, while the IT infiltrating zone composition was 10–20 tumor cells per visual field, and the CT tumor zone contained an average of 300/1 ratio of tumor cells to normal cells. The PAN and PNZ zones were defined by aggregation of nuclei around necrosis with or without pseudopalisading cells respectively. And the HBV and MVP zones were distinguished by blood vessels with either hypertrophic thickened walls or sharing endothelial walls respectively.

Molecular validation of some Epi358 genes

The expression of only 9 of the Epi358 genes in the Ivy database have been validated by ISH at the LE and despite the uniform molecular genetic procedures used to build this database and evidence of clear segmentation in 6 of these genes (Figure S5), extended analysis could reveal anomalies in compartmental values. In future studies, single cell RNAseq analysis of spatial samples will provide validation as well as the identity of neuronal and glial subtypes for each gene.

Further genetic inclusion and exclusion criteria

Per the revised definition of glioblastoma published by the World Health Organization in 2021,[103] we omitted samples derived from patients with IDH1/2 mutation, resulting in the exclusion of four patients. To facilitate interpretation of regional tumor mechanisms, we also excluded tumors which were derived from multiple lobes in the brain ($n = 6$ patients excluded), resulting in a total of 163 samples from 29 patients which were each probed for 25,873 genes. A summary of the number of patients and samples collected for each region of the tumor and full methodological details are available at the Allan Brain Atlas/Ivy GAP website: https://help.brain-map.org/display/glioblastoma/Documentation.

Calculation of enrichment ratio per tumor region

The enrichment ratio is an intra-tumoral comparison which highlights tumor heterogeneity and can be used to identify genes enriched per tumor region. Regional RNA-Seq was downloaded from Ivy GAP[19] database, and samples were segregated by tumor lobar location. Per frontal, temporal, and parietal lobar locations, the enrichment ratio was calculated for six anatomically defined tumor regions LE, IT, PNZ, PAN, HBV, and MVP as compared to expression levels at the CT. We defined an ER of $\geq$1.5-fold as enriched in the region of interest (ROI) as compared to the CT, and an ER of $\leq$0.5 as enriched in the CT compared to the ROI.

$$ER_{region\ of\ interest} = \frac{Avg\ RNA_{region\ of\ interest}}{Avg\ RNA_{\ pure\ tumor\ cell\ region}}$$

In order to compare the enrichment ratios across cortical regions, we determined that the relative expression of the Epi358 genes did not vary greatly amongst the frontal, temporal, and parietal lobes in healthy adult brain (Figure S6, lane 1). Comparison of the tumoral enrichment ratios per lobe demonstrated that the majority of genes also showed a similar enrichment ratio regardless of cortical regions (Figure S6, lanes 2–6). Due to the high congruence of enrichment ratios from tumors derived from different cortical regions, we display the average enrichment ratio across the frontal, temporal, and parietal lobes per tumor region in Figure 1A.

To display the heterogeneity within the cellular tumor, we calculated the enrichment ratio of the average RNA of all samples per patient for each region of the tumor as a function of the lobar-matched average expression of the cellular tumor.

$$ER_{per\ patient} = \frac{RNA_{patient\ X}}{Avg\ RNA_{\ Lobar\ matched\ CT}}$$

Calculation of case concordance

We used the coefficient of variation (stdev/average) as a measure of case concordance and defined a low concordance as a CV $\geq$ 0.50, a high concordance as a CV $\leq$ 0.25, and a medium concordance as intermediate values between 0.25 and 0.50. Regional RNA-Seq was downloaded from Ivy GAP database, and TCGA bulk RNA-Seq was downloaded from the Human Protein Atlas website. The coefficient of variation was first determined per lobar location before averaging for the final coefficient of variation displayed in Figure 1.

$$Coefficient\ of\ Variation\ (CV) = Avg(CV_{FL}, CV_{TL}, CV_{PL})$$

Calculation of fold Change between cases with and without seizures (FC_{sz}):

We stratified the Ivy GAP RNA-Seq according to patient history, forming two groups, cases with seizures and cases without seizures. We then determined the fold change between these two groups per tumoral region.

$$FC_{sz} = \frac{Avg\ RNA_{seizure\ cases}}{Avg\ RNA_{\ non-seizure\ cases}}$$

Hierarchal clustering of the Epi358 genes into functional groups based on biological process

To hierarchically cluster the Epi358 genes based on their biological processes listed in the Gene Ontology Database, we used the *godata* function of *GOSemSims* R Package to generate a semantics similarity database for the Biological Processes (BP GO) of human genes listed in the Gene Ontology Database. The *mgeneSim* function from the *GOSemSim* package was then used to calculate the pairwise semantic similarities of the Epi358 genes based on their BP GO semantic annotations using the Wang method.[104] The *hclust* function from the *STATS* package in R was then used to hierarchically cluster the Epi358 genes based on BP GO semantics similarity matrix scores using the ward.D method. Hierarchical clustering was successful for 349/358 Epi358 genes, resulting in 3 major clusters. We conducted a GO over-representation analysis[105] of the BP for each of the clusters using the *clusterProfiler* package[106] to assign the major categories displayed in Figure 1: (1) Cell Growth and Division; (2) Ion Channel and Transport; (3) Macromolecule Biosynthesis. The hierarchal cluster was then converted into a phylo object used for phylogenetic analysis in R using the *as.phylo* function in the *tidytree* package.[107] The phylogenic object based on the BP GO of the Epi358 genes were then visualized using *ggtreeExtra* package[107] in R as a fan tree diagram with an open angle of 30°. For the circular dendrogram in Figure 1, we annotated the circular dendrogram with the ER and CV per tumor region using the *geom_fruit*, and *geom_tile* function in *ggtreeExtra*.

Calculation of fold change of epilepsy genes at the peritumoral LE vs. healthy cortex

To compare LE expression to healthy human brain, we downloaded region matched healthy human cortical RNA-Seq datasets from the Allen Brain Institute Brain Span Project[108] and the Human Protein Atlas[25] Brain and Pre-frontal Brain Gene Data. To compare LE and cortical tissue RNA-Seq across different datasets, we normalized all genes by five genes which showed invariant expression across multiple cortical regions in both the Allen Brain Atlas and Human Protein Atlas healthy cortical datasets (*RNF10, M6PR, AIFM1, APEX1, CNDP2*). We determined the expression fold change for each lobar location of the derived LE (i.e., FL, TL, PL), as well as the pooled cortical sample (Cx), which included gene expression at the frontal lobe, temporal lobe, and parietal lobe.

$$FC_{Cx} = \frac{Avg\ RNA_{LE\ per\ FL,TL,or\ PL}}{Avg\ RNA_{\ Healthy\ Fl,TL,or\ PL}}$$

To determine the congruence across the ER and FC across the FL, TL, and PL, we categorized the data roughly into those with ERs or FCs >1.5, <0.5, or between those two threshold values, assigning them as enriched, under-enriched, no change for ERs and then upregulated, downregulated, no change for FCs. The categorized variables were then sorted for genes which showed identical categorical ERs and/or FCs, forming 15 groups displayed in Figure 2.

Identification of pathogenic copy number variants that are epilepsy linked

A prior study conducted a meta-analysis of rare copy number variants on the 22 autosomes, cumulating data from 17 different sources.[109] We extracted data from this resource and determined which genes located on these rare copy number variants were clinically validated as epilepsy linked, resulting in a panel of 41 genes. We then determined the ER and FC_{Cx} for these epilepsy-linked genes located within pathogenic copy number variants.

Curation of gene set of disease-linked genes and presynaptic genes

Relevant epilepsy linked genes were compiled from a diagnostic panel of 320 genes (https://www.invitae.com/en/providers/test-catalog/test-03401) and recent literature, resulting in 358 epilepsy/dysplasia-linked genes (Table S1). Dysplasia/cortical malformation genes were identified from a panel of genes linked to malformations of cortical development.[79] Presynaptic genes were curated from the literature for genes involved in the cytoskeletal matrix assembled at the assembly zone (CAZ), SNARE family proteins including synaptotagmins (SYT) and synaptobrevins (VAMP), synaptic vesicle proteins such as clathrin and syntaxins, and adaptor proteins which may regulate synaptic vesicle composition (AP complexes). In addition, murine gene ontology annotations for synaptic exocytosis processes (GO:0140029) was included for further consideration if involved in priming, docking, fusion or targeting of synaptic vesicles.

Comparison of FC_{Cx} at the LE to expression levels during healthy early development

Human RNA-Seq at the frontal, temporal, and parietal lobes for different developmental stages was downloaded from the Allen Brain Institute BrainSpan Project (https://www.brainspan.org/).[108] To make comparisons across the BrainSpan and HPA RNA-Seq datasets, we first normalized the BrainSpan data to adult cortical levels within the BrainSpan dataset (Adult.A). Next, we normalized Adult.A levels from BrainSpan and Adult.B expression levels from HPA using five genes which showed invariant expression across multiple cortical regions in both the Allen Brain Atlas and Human Protein Atlas healthy cortical datasets (*RNF10, M6PR, AIFM1, APEX1, CNDP2*). A ratio was formed using normalized Adult.B/Adult.A levels per cortical lobe. We then determined the FC_{Cx} compared to healthy adult cortex for each early developmental stage per FL, TL, and PL using the equation for FC_{cx} below. Due to the high congruence of expression of Epi358 genes across the FL, TL, and PL, we displayed the average FC_{Cx} for these three lobes in Figure 5.

$$FC_{Dev.norm} = \frac{Avg\ RNA_{Dev\ Stage\ per\ FL,TL,or\ PL}}{Avg\ RNA_{\ Adult.A\ per\ FL,TL,or\ PL}}$$

$$FC_{Adult.norm.ratio} = \frac{Avg\ RNA_{Adult.B\ per\ FL,TL,or\ PL}}{Avg\ RNA_{\ Adult.A\ per\ FL,TL,or\ PL}}$$

$$FC_{Cx} = \frac{FC_{Dev.norm\ per\ FL,TL,or\ PL}}{FC_{\ Adult.norm.ratio\ per\ FL,TL,or\ PL}}$$

Overrepresentation analysis of development related functions

The Epi358 genes were stratified into genes which were upregulated and downregulated per LE and early developmental stage, forming 10 expression groups. We then conducted a Gene Ontology over-representation analysis[105] of the biological process for each of the expression groups using the *clusterProfiler* package.[106] A significance level of less than 0.05 for the adjusted *p*-value was used to filter for significant results. We then prioritized developmentally relevant Gene Ontology terms involved in growth signaling, migration, and pre- and post-synaptic functions.

Prioritized GO terms:
Growth signaling: GO:0032007.
Migration: GO:0001764.
Presynaptic Function: GO:0042391, GO:0007416, GO: 0099003.
Postsynaptic Function: GO: 0099565, GO: 0060079.

Determination of cortical developmental index for fold changes compared to WT

The Cortical Developmental Index (CDI) is a modified strategy for comparing developmental stages which was previously tested in fast-spiking interneurons[110] and microglia.[111] The CDI normalizes expression across different stages so that the condition with a zero CDI score represents the minimum value of all the tested conditions and a score of 1 equals the maximum CDI value of all the conditions tested. To facilitate comparison across Ivy GAP LE and BrainSpan datasets, we normalized FL expression by genes which showed invariant expression across all developmental stages at the FL (*ARFGAP2, BSDC1, DMAP1)*. The CDI was then determined for the normalized expression at LE samples derived from the FL and normalized FL expression in healthy cortex from various developmental stages.

$$CDI = \frac{FC_{x_{stage}} - FC_{x_{minimum\ across\ all\ stages}}}{FC_{x_{maximum\ stage}} - FC_{x_{minimum\ across\ all\ stages}}}$$

QUANTIFICATION AND STATISTICAL ANALYSIS

An unpaired two-sample t-test and Welch's t-test was used to determine statistical significance of intratumoral enrichment ratio for samples with and without equal variances respectively. A threshold *p*-value of 0.05 was used to determine statistical significance.